CHARACTERIZATION OF CHOLESTEROL TARGETING ANTIMICROBIAL PEPTIDES AND ASSESSMENT OF THEIR ANTIVIRAL ACTIVITY *IN VITRO*

by

Mary Louise Hasek

B.S., University of Pittsburgh, 2012

Submitted to the Graduate Faculty of

the Department of Infectious Diseases and Microbiology

Graduate School of Public Health in partial fulfillment

of the requirements for the degree of

Master of Science

University of Pittsburgh

2014

UNIVERSITY OF PITTSBURGH

GRADUATE SCHOOL OF PUBLIC HEALTH

This thesis was presented

by

Mary Hasek

It was defended on

June 25, 2014

and approved by

Phalguni Gupta, PhD
Professor
Department of Infectious Diseases and Microbiology
Graduate School of Public Health
University of Pittsburgh

Todd Reinhart, ScD
Professor
Department of Infectious Diseases and Microbiology
Graduate School of Public Health
University of Pittsburgh

Thesis Director:
Ronald Montelaro, PhD
Professor
Department of Microbiology and Molecular Genetics
School of Medicine
University of Pittsburgh

Ronald Montelaro, PhD

CHARACTERIZATION OF CHOLESTEROL TARGETING ANTIMICROBIAL PEPTIDES AND ASSESSMENT OF THEIR ANTIVIRAL ACTIVITY *IN VITRO*

Mary Hasek, M.S.

University of Pittsburgh, 2014

ABSTRACT

In recent decades, efforts have been made to rationally design antimicrobial peptides (AMPs) for use as alternative therapeutics. The *de novo* designed AMP WLBU2 is a 24 residue long cationic, α-helical peptide. Antimicrobial activity of WLBU2 is predicted to be based on peptide interaction with lipid membranes leading to bilayer disruption. Antibacterial activity of WLBU2 has been displayed against a wide-range of antibiotic resistant Gram positive and Gram negative bacteria based on charge interactions between the cationic peptide and the anionic bacterial membrane lipids. Preliminary experiments indicated WLBU2 has antiviral activity against various enveloped viruses suggesting the potential for development of a broad spectrum antiviral treatment. While viral envelopes do not have the same negative surface charge presumed to be the basis for antibacterial activity of WLBU2, most mammalian virus membranes are enriched for cholesterol relative to host cells. We hypothesized that specifically targeting WLBU2 to cholesterol rich membranes would increase antiviral activity against a broad range of enveloped mammalian viruses. Addition of the cholesterol recognition amino acid consensus (CRAC) motif is predicted to direct WLBU2 to cholesterol rich viral envelopes, thereby disrupting the membrane and leading to virus inactivation. When tested against human immunodeficiency virus (HIV), influenza A, and dengue virus (DENV), computationally designed CRAC motif

containing peptides and unmodified WLBU2 activity varied across the panel of viruses tested. Antiviral activity was observed against influenza A and DENV, and CRAC motif containing peptides were about 10-fold more effective against DENV than unmodified WLBU2. Therapeutic indices of CRAC motif containing peptides were similar to that observed for unmodified WLBU2. These findings suggest that AMPs can be designed to enhance antiviral activity, representing a novel therapeutic design with the potential for significant public health impact against global diseases such as influenza and DENV.

TABLE OF CONTENTS

LIST OF TABLES

LIST OF FIGURES

ACKNOWLEDGEMENTS

First, I would like to thank my thesis advisor, Dr. Ron Montelaro, and my committee members, Dr. Phalguni Gupta and Dr. Todd Reinhart, for the opportunity to learn and grow to become a better scientist. I would like to thank all the members of my lab, especially Jonathan Steckbeck and Toni Deslouches, for their input and advice along the way. I would like to extend my sincere gratitude to my classmates for their support throughout navigating this portion of our educations. I would like to thank my roommates and friends, especially Greg Vose and Kim Coopperrider, for their love, support, and levity; you all have faked more interest in my work than I ever could have asked for. And most importantly, I would like to thank my family for their unconditional love and support and their shipments of fresh roasted coffee on demand.

1.0 INTRODUCTION

In the past decade, antimicrobial peptides (AMPs) have been considered for their potential as novel therapeutic agents against bacteria, viruses, and fungi. Naturally occurring AMPs are produced by animals and plants as important components of the first line of defense of the innate immune response (1; 2). They have evolved to respond to properties of microbes that are not dependent on metabolic activity, allowing for a broader range of antimicrobial activity based on general membrane properties that are similar between most microbial membranes (3). Because of this, AMPs have been designed, developed and tested for treatment against bacteria, viruses, fungi, and even cancer.

1.1 NATURALLY OCCURRING ANTIMICROBIAL PEPTIDES

While over 2000 AMPs have been identified from various plants and animals (4), some general properties have been observed that allow for peptides to disrupt or traverse membranes. AMPs are commonly made of fewer than 100 amino acids (32 amino acids average), have a net cationic charge, and form an amphipathic structure where positive residues segregate to one side and hydrophobic residues to the opposite (5). Almost all identified AMPs can be categorized into four major classes based on peptide structure: β-sheet, α-helical, extended, and loop peptides (Figure 1) (6). The range of AMP structures and sequences likely reflects the specialization of

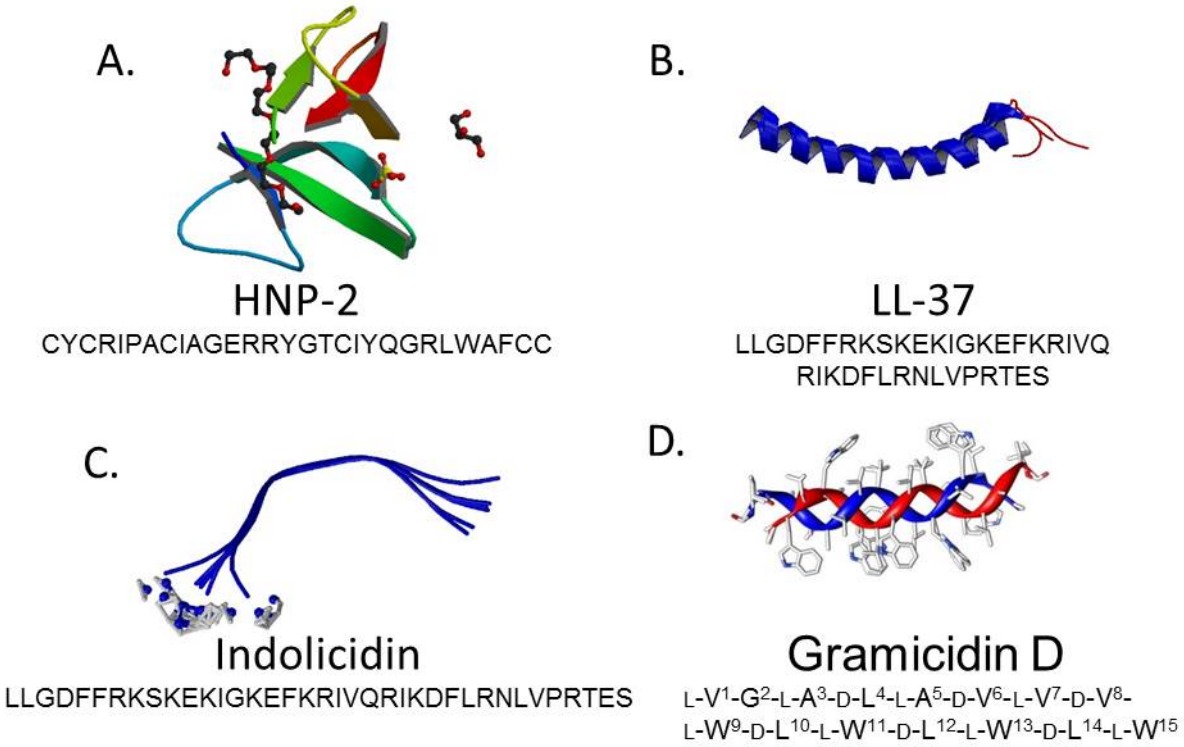

A. β-sheet peptides represented by the defensin human neutrophil protein-3 (10.2210/pdb1zmh/pdb). **B.** α-helical peptides represented by the human cathcathelicidin hCAP-18/LL-37 (10.2210/pdb2k6o/pdb). **C.** Extended peptides as represented by bovine indolicidin (10.2210/pdb1g89A/pdb). **D.** Loop peptides as represented by gramicidin dimer from *Brevibacillus brevis* (10.2210/pdb1bdw/pdb). All structures obtained from RCBS PDB (www.rcsb.org/pdb/home/home.do).

Figure 1. The four major classes of antimicrobial peptides represented structurally by one member of each class.

each peptide to different environments in the body (7). In humans and other mammals, two of the most important classes of AMPs produced within the body are the defensins and cathelicidins which fall into the β-sheet and α-helical peptide structural classes, respectively. Defensins and cathelicidins are generally distributed throughout the epithelia and mucosa and are present constitutively at relatively high concentrations (8). Though structurally distinct, both defensins

and cathelicidins are important in the innate immune response to infection, as evidenced by their wide distribution and ubiquitous presence (8; 9).

Most AMPs, including defensins and cathelicidins, exploit natural properties of target membranes to distinguish self from non-self and cause permeabilization of target membranes (3; 10). The cationic charge and amphipathic structure of AMPs allow for specific targeting of foreign membranes based on differences in lipid composition, as best characterized by their antibacterial activity (10). The outermost leaflet of bacteria contains more anionic lipids than animal cell membranes, thus AMPs target bacterial membranes specifically based on surface charge. Once attracted to the foreign membrane, AMPs assume an amphipathic structure where hydrophobic residues insert into the membrane based on interactions with the non-polar tails of lipid bilayers (Figure 2). Peptide interaction with the membrane can lead to disruption through

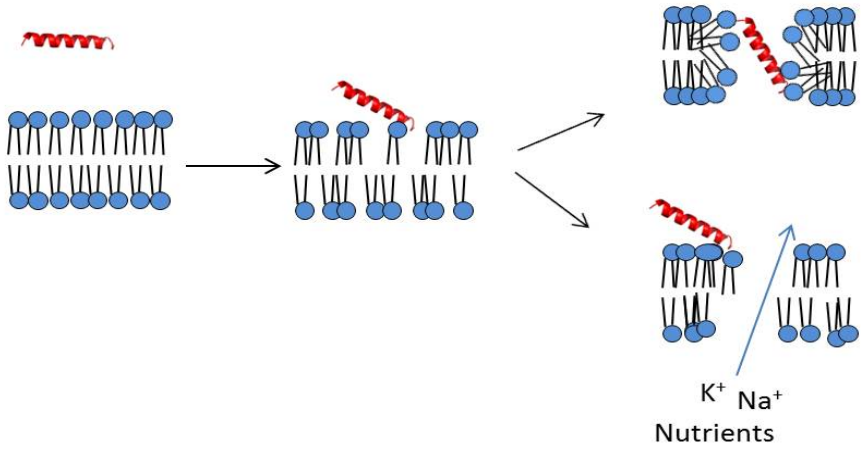

Initial contact between ordered lipid bilayer and AMP occurs through cationic residue interaction with phospholipid head. This interaction disrupts the membrane as hydrophobic residues insert into the bilayer disordering the membrane. This disorder allows peptide to either form pores in the membrane or cross into the cell.

Figure 2. General mechanism of action for AMPs.

various proposed mechanisms, including barrel-stave, carpet, and toroidal pore mechanisms (11). In each of these mechanisms, peptides aggregate in different conformations at the surface of the membrane and cause permeabilization through interaction of these peptide aggregates with the membrane surface. Evidence towards each of these mechanisms exists, yet it does not appear that any one is specific to a particular peptide class (12). Further, it is possible that the same peptide could disrupt membranes through all of these mechanisms based on the interaction with a particular membrane (3). AMPs can then cause death or inactivation either by leading to efflux of ions and essential nutrients or by entering the cell and interacting directly with intracellular components (5). AMPs have even been considered for their potential as anticancer treatments based on these similar membrane targeting strategies (13; 14). AMPs have emerged as an attractive antimicrobial alternative because they target fundamental membrane characteristics that are difficult for bacteria, viruses, and fungi to alter and still remain viable and infectious.

1.1.1 LL-37

Since its initial discovery in 1994 (15), the human cathelicidin LL-37 has been extensively studied for its therapeutic potential in treating bacterial, viral, and fungal infections. This naturally occurring α-helical peptide is 37 amino acids long and is known to be an important component of mucosal immunity, most importantly in the lung (8). LL-37 also possesses various other functions including immune modulation, apoptosis, and chemotaxis (16). It is produced from a precursor peptide known as hCAP-18 by proteolysis in neutrophils, macrophages, and some epithelial cells (17). Antibacterial and antiviral activity against a broad range of pathogens has been demonstrated using LL-37 in *in vitro* culture conditions. Further, LL-37 has also demonstrated antiviral activity against various enveloped viruses, including

influenza A (18), herpesviruses (19), vaccinia (20; 21), human immunodeficiency virus (HIV) (22), adenovirus (23), and respiratory syncytial virus (RSV) (24) *in vitro*. In the case of influenza A, LL-37 likely exerts its antiviral activity by membrane disruption (25), whereas for HIV, it has been proposed that infection is blocked by direct interaction with reverse transcriptase, inhibiting replication (26).

Despite the broad range of activity of LL-37, there are limitations to its use as a potential therapeutic. In *in vitro* studies, the antimicrobial activity of LL-37 varies widely based on conditions such as serum and salt concentrations, as well as pH (16). These conditions also vary across different environments in the body, indicating that LL-37 is best suited for activity within the lung and would be less effective in other parts of the body, such as the blood or gastrointestinal tract (8). Concentrations of LL-37 are elevated in the lungs of cystic fibrosis (CF) patients where there are chronic bacterial infections, leading to a persistent inflammatory environment (27). However, abnormally high salt concentrations, reduced airway surface pH (28), and complexation with glycosoaminoglycans (29) diminish the antimicrobial potential of LL-37 associated with the respiratory epithelium. Indeed, these deficiencies in LL-37 activity in the CF lung are thought to contribute to the ability of bacteria to easily colonize the lung. These observations indicate that the environments in which AMPs are naturally found affect the activity of those peptides. Due to the limitations of application for LL-37 as a potential antimicrobial, efforts have been made to design *de novo* AMPs that would have a similarly broad range of antimicrobial activity without the limitations observed in certain pH and salt conditions.

1.2 ENGINEERED CATIONIC ANTIMICROBIAL PEPTIDES – WLBU2

Using observations of the properties of naturally derived AMPs, engineered cationic AMPs have been developed as therapeutics by multiple labs (30; 31; 32). In the past decade, our lab has been at the forefront of engineering AMPs based on structural and functional characteristics of host-derived peptides with potent antimicrobial activity (33; 34). Our lab previously designed and characterized a series of peptides based on the lytic base unit (LBU) of 12 amino acids composed of arginine and valine (35). The LBU was designed to form an idealized amphipathic helix in which all cationic residues segregate to one side and all hydrophobic residues to the other. These peptides were also designed to take advantage of the cost effectiveness of condensation chemistry to combine LBUs into a series of peptides of various lengths. Maximal activity was observed at 24 residues, similar to the average length of 32 residues observed in naturally occurring AMPs. Because previous experiments had shown that tryptophan increases antimicrobial activity of peptides (36; 37; 38), valine residues of the LBU were replaced with tryptophan residues, producing a series of WLBU peptides of various lengths (35). From this series of peptides, WLBU2 had emerged as our frontrunner peptide based on its broad range of activity (Figure 3). WLBU2 forms a helix with a higher hydrophobic moment than LL-37 and it forms a more perfectly amphipathic structure, indicating that rational design can create AMPs with idealized structural properties.

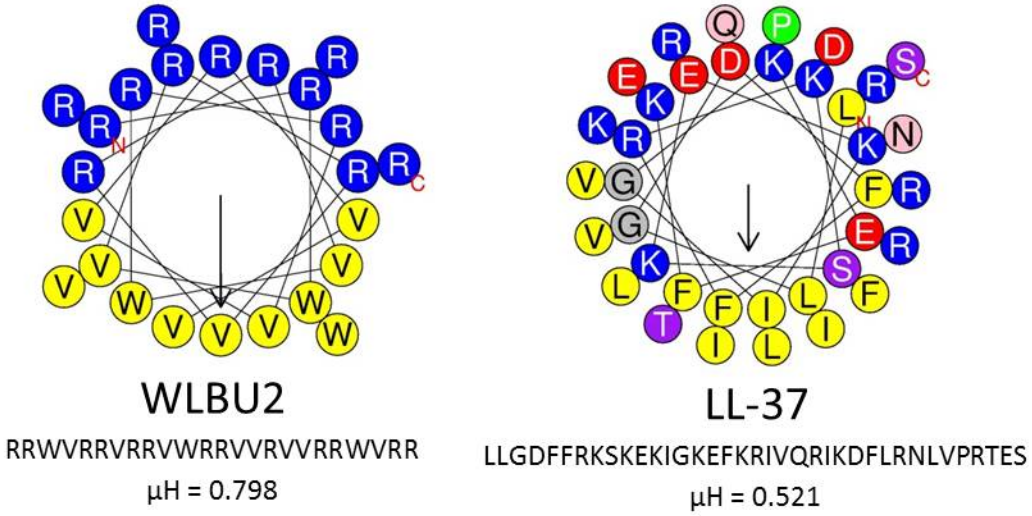

Hydrophobic residues are shown in yellow and cationic residues are shown in blue. The direction of arrow represents hydrophobic moment (μH), with the length of the arrow indicating strength.

Figure 3. Helical wheel models comparing hydrophobic residue segregation of WLBU2 against LL-37.

WLBU2 has been studied for its antibacterial activity *in vitro* against a wide range of Gram positive and Gram negative bacteria. Antibacterial activity has been observed in sub-micromolar concentrations for various strains of *Pseudomonas* and *Staphylococcus* in various salt concentrations, outperforming LL-37 in the same assays to measure minimum bactericidal concentration (MBC) and minimum inhibitory concentration (MIC; Table 1) (35; 39). Furthermore, WLBU2 has been shown to have activity against other pathogenic bacteria, including *Burkholderia, Enterococcus,* and *Acetinobacter,* as well as some pan-resistant strains (40). Interestingly, WLBU2 retains activity in high salt, serum, and whole blood environments, in which LL-37 has little to no detectable activity (39; 41). This indicates that the rational engineering of peptides can overcome the natural limitations of host-derived peptides. WLBU2

has also displayed antiviral activity in preliminary experiments *in vitro* and *in vivo* against a variety of mammalian enveloped viruses. Antiviral activity was detected against HIV

Table 1. MBC and MIC values for *P. aeruginosa* strain PAO1 and methicillin-resistant *S. Aureus* (MRSA) in phosphate buffer (PB), PB containing 150 mM NaCl (PBS), and Mueller-Hinton broth (MHB).

	PAO1			MRSA		
	MBC* (μM)		MIC† (μM)	MBC* (μM)		MIC† (μM)
	PB	PBS	MHB	PB	PBS	MHB
WLBU2	0.6	0.6	4	0.6	0.6	2
LL-37	1.2	1.2	8	1.2	6	>32

*MBC measured as concentration of peptide reducing viable bacteria within a suspension by three orders of magnitude.
†MIC measured as concentration reducing bacterial growth by at least 90%.

and influenza A. Mice infected with a 70% lethal dose of influenza A strain PR8 were able to survive disease when treated with WLBU2 intranasally (results not published). Based on these data, WLBU2 can potentially be developed for use as a broadly active antiviral peptide. In principle, this is an attractive idea because antiviral treatments currently available are virus-specific. By increasing peptide specificity for properties of viral envelopes shared among various families of viruses, the antiviral activity of WLBU2 could be increased against a variety of mammalian enveloped viruses that are significant public health threats.

1.3 CRAC MOTIFS

Specifically targeting viral envelopes is difficult because the phospholipid profiles of viral and host cellular lipid membranes are similar. However, studies of viral envelopes have identified an increase of the cholesterol-to-phospholipid (C/P) ratio as compared to the host membranes from which they are derived. This cholesterol enrichment has also been shown to be necessary for virus infectivity (42). An amino acid sequence called the cholesterol recognition amino acid consensus sequence (CRAC) motif can direct proteins to cholesterol-rich membranes (43), representing a plausible targeting strategy for enveloped virus inactivation. The CRAC motif is a flexible sequence of anywhere from 5 to 13 amino acids that directs proteins to cholesterol rich regions of membranes. The consensus sequence is L/V – X(1-5) – Y – X(1-5) – R/K, in which X(1-5) represents one to five residues of any amino acid (44). This motif is thought to function by stably interacting directly with a cholesterol molecule by stacking of aromatic groups (43). It appears proper CRAC function relies on structural flexibility of the motif to allow for stable and specific interaction with cholesterol (45). There are millions of possible CRAC motif sequences, though it is likely that not all lengths and sequences are equally efficient. Studies have shown that making single amino acid changes or additions in an established CRAC motif sequence can alter cholesterol specificity (45).

One well studied CRAC motif is LWYIK found in HIV gp41. This is the shortest possible CRAC motif, and its activity has been well characterized. Single amino acid mutations to the first, third, and fifth residues of LWYIK have shown that these residues are most important for efficient interactions with cholesterol (45). This also revealed that drastic changes could be made to the rest of the sequence with little to no effect on cholesterol interactions. Other work with the LWYIK CRAC motif in the context of HIV gp41 has revealed that this sequence inserts

specifically into the cholesterol-enriched viral envelope to encourage destabilization of the membrane and to allow for fusion with the host cell (46; 47). These studies indicate that CRAC motifs could be designed to follow the appropriate sequence that could interact specifically with cholesterol rich membranes.

1.4 SELECTED MODEL VIRAL MEMBRANES

For this study, three viruses were selected against which CRAC motif containing peptides were tested for their ability to inactivate infection. These viruses, each from different virus families, were chosen to represent a spectrum of lipid:protein content and lipid surface exposure in the viral envelope. The following viruses also represent significant contributors to global morbidity and mortality caused by viral disease.

1.4.1 Human Immunodeficiency Virus

HIV is a recently emerged lentivirus that can lead to acquired immune deficiency syndrome (AIDS), a disease characterized by impaired immune function leading to fatal opportunistic infections. There are currently no vaccines against HIV, though quality of life after infection can be maintained for decades through antiretroviral therapies. The World Health Organization (WHO) estimated that as of 2012, 35.3 million people were currently infected with HIV, with 2.3 million new infections occurring within that year. During this period from its discovery in 1983 to 2012, the WHO estimates 36 million people have died of HIV and HIV-related complications (48).

The HIV virion is enclosed in a host-derived lipid envelope surrounding a proteinaceous capsid that protects the viral genome (Figure 4a). The virus membrane is studded with about 7 to 14 copies of the virally-derived envelope (Env) trimer consisting of gp120 and gp41 (49). The lipid bilayer has been shown to be derived specifically from detergent-resistant, cholesterol and sphingomyelin rich regions of the host cell membrane, sometimes called lipid rafts (50). Studies of the composition of the HIV envelope have revealed that the viral membrane has a significantly higher cholesterol:lipid ratio than corresponding host cell membranes, with C/P ratios ≥ 0.8 in both clinical and laboratory isolates (51), whereas human skin fibroblasts have a C/P ratio of about 0.15 in normal growth media conditions (52). Furthermore, the presence of cholesterol in the viral envelope has been shown to be necessary for proper fusion, while cholesterol depletion significantly reduces infection (53; 54). In the context of testing cholesterol targeting AMPs, the HIV virion models a membrane with low protein density and high surface lipid exposure.

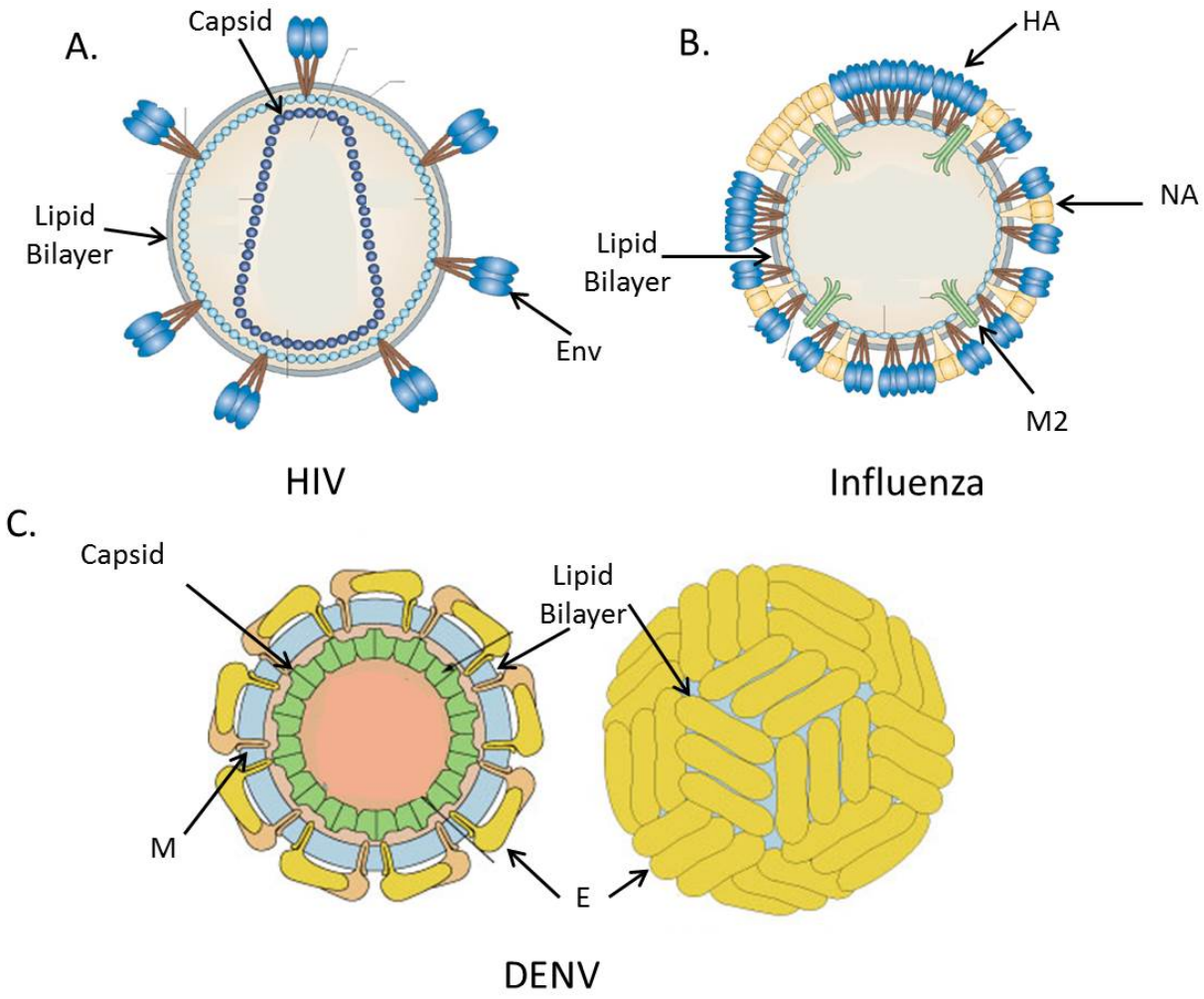

A. HIV model showing lipid bilayer and approximately 7 Env trimers on the surface of the virion. Model is adapted from **(105)**. **B.** Influenza model showing lipid bilayer studded with multiple copies of HA and NA with less surface lipid exposure as compared to the HIV model. Model is adapted from **(105)**. **C.** DENV model showing both a cutaway to the interior of the virion as well as a model of the outer surface covered by icosahedral shell of E protein. Model is adapted from **(106)**.

Figure 4. Schematic diagra ms of panel of viruses chosen to test CRAC motif containing peptides against.

1.4.2 Influenza A Virus

Influenza A virus is an orthomyxovirus that causes respiratory illness in yearly seasonal pandemics. Influenza-associated hospitalizations and mortality most severely impact the elderly (65+ years old) and juvenile (<5 years old) age groups (55). For the 2003 United Stated influenza season, a moderately severe season, the total economic burden of the epidemic is estimated to have cost about $87.1 billion and resulted in 44 million productive days lost due to illness or death, representing a significant public health threat to the US (56). The WHO established the Global Influenza Surveillance Network (GISN) to monitor global trends of influenza disease, allowing for the annual production of influenza vaccines against current circulating strains (57). However, influenza A can mutate rapidly within humans, birds, and pigs, leading to emergence of new virulent strains of influenza A to which the human population has no natural immunity (58). The recent emergence of avian virus H5N1, which has been shown to cause disease in humans, provides an ongoing example of the mutagenic potential to create new epidemic strains of virus (59). Currently, there are few antiviral therapies against influenza A, though some including oseltamivir and zanamivir do exist (60).

The influenza A virion is a spherical or filamentous particle enclosed in a lipid membrane that surrounds eight RNA segments wrapped around and protected by the nucleocapsid protein. The viral membrane is studded with three different virally derived proteins: hemagglutinin (HA), neuraminidase (NA), and M2 matrix protein (Figure 4b) (61). During assembly, these three proteins will assemble specifically in areas of the membrane that are insensitive to detergent solubilization, a defining property of lipid rafts (62). The lipid composition of the viral envelope matches that of ordered lipid raft domains of mammalian cells and indicates that increased cholesterol content of the envelope is necessary for infection. Studies of purified virus particles

have determined that 44% of envelope lipid is cholesterol, accounting for about 12% of the total virion mass (63). Studies of the surface of the 2009 pandemic H1N1 virus have indicated that even though there is a relatively high surface expression of HA and NA proteins, antibodies are still able to access the stem regions of HA that are close to the viral membrane, indicating that there is accessibility to the lipid envelope (64). In the context of testing cholesterol targeting AMPs, the influenza A virion models a membrane with high protein density and moderate surface lipid exposure.

1.4.3 Dengue Virus

Dengue virus (DENV) is an acute mosquito-borne virus of the Flavivirus family that is endemic in tropical and sub-tropical regions of the globe, especially South East Asia and Africa. DENV is considered the most important arboviral disease globally by the WHO because 50% of the world's population lives in countries where the disease is endemic (65). Infection causes multiple disease outcomes of varying clinical severity: Dengue fever (DF), Dengue hemorrhagic fever (DHF), and Dengue shock syndrome (DSS). In the past decade, more countries have reported increasing cases of DF or DHF due to issues such as global travel, climate change, and breakdown of vector control mechanisms (66). Recent estimates on the number of people infected globally per year approximate 390 million new infections with 96 million clinical manifestations of disease (67). In most endemic countries, children constitute most of the burden of mortality (68). Currently, there are no vaccines or specific antiviral treatments against DENV infection.

The DENV virion is distinct from that described for HIV and influenza A. The DENV genome is protected by an inner nucleocapsid protein that is then surrounded by a capsid. This

capsid is then surrounded by a host derived lipid membrane. Distinct from both HIV and influenza A, the DENV lipid envelope is further protected by an icosahedral shell formed by 90 copies of the E protein dimers, embedded in the membrane by complexation with the M protein (Figure 4c) (69; 70; 71). Similar to HIV and influenza A, recent studies have shown that assembly of DENV is dependent on lipid raft regions where depletion of cholesterol from the host cell leads to decreased virus production (72). Though there have been no studies to directly measure how much cholesterol is present in the DENV envelope, it has been shown that depletion of cholesterol from the viral envelope reduces viral infectivity, indicating an essential role for cholesterol in the viral membrane (73). Given these observations, the DENV virion represents a model where the viral envelope has a very high protein:lipid ratio and very low lipid surface exposure.

Based on the observation that many mammalian viral envelopes are enriched for cholesterol as compared to host cell membranes, we hypothesized that AMPs could be developed as antiviral agents by specifically targeting cholesterol-rich membranes. We hypothesized that addition of CRAC motifs to WLBU2 would increase peptide specificity for cholesterol-rich membranes intrinsic to enveloped mammalian viruses. These CRAC motif-containing peptides would interact with viral envelopes based on the different C/P ratios as compared to the host cells, thereby presenting a new strategy of antiviral treatment against a broad range of mammalian viruses. We predicted that viral inactivation by CRAC motif containing peptides would correlate to lipid surface exposure based on a membrane disruptive mechanism of action.

2.0 STATEMENT OF PURPOSE

Enveloped viruses, including HIV, influenza, and flaviviruses, are a significant cause of morbidity and mortality across the globe. There are few effective antiviral therapies that exist and those that do are highly pathogen-specific, often developed with the intent to treat one specific virus. One problem with this form of treatment is the ability to develop resistance mechanisms to the drug. Therefore, there is a critical need to develop novel therapeutics that have a broad range of activity and are difficult for resistance to be developed.

In the past two decades, AMPs have been extensively studied and developed for their use as antibacterial agents. While antiviral activity has been examined for some naturally-derived peptides, little work has been done to specifically engineer peptides as antiviral agents. The engineered cationic antimicrobial peptide WLBU2 developed by our lab has demonstrated in preliminary experiments the ability to inactivate enveloped mammalian viruses, through a presumed membrane disruptive mechanism. The goal of this work was to determine whether the antiviral activity of WLBU2 could be increased by the addition of the CRAC motif in order to direct peptides specifically to cholesterol-rich membranes. Because viral envelopes are enriched for cholesterol as compared to host mammalian cells, we hypothesized that addition of the CRAC motif would direct WLBU2 specifically to viral envelopes, disrupting the membrane and therefore inactivating virus and blocking infection. This marks a novel antiviral strategy in which

entire classes of viruses can be targeted by a mechanism in which viruses are unknown to be able to develop resistance.

2.1 SPECIFIC AIM 1: TO DESIGN, MODEL, AND CHARACTERIZE CRAC MOTIF CONTAINING PEPTIDES.

Because the CRAC motif is a domain with millions of possible amino acid sequences, motifs will be designed for addition to WLBU2. In order to determine the optimal location for addition of CRAC motifs to WLBU2, modeling will be carried out to predict the structures of C- and N-terminal CRAC motif containing WLBU2 peptides. Once peptides are produced with the appropriate CRAC motif additions, peptides will be characterized by circular dichroism (CD) spectroscopy in various solvent environments and analyzed for secondary structure composition.

2.2 SPECIFIC AIM 2: TO EVALUATE ANTIVIRAL ACTIVITY OF THESE PEPTIDES AGAINST VARIOUS ENVELOPED VIRUSES *IN VITRO*.

CRAC motif containing peptides will be tested for their antiviral activity against the following enveloped mammalian viruses: HIV, influenza A, and DENV. This panel of viruses was chosen because they represent a range of membrane protein concentrations and lipid surface exposures. Peptides will be tested against each virus in the appropriate infection assays to measure how pre-treatment of virus with peptide affects infectivity. These measures of

inactivation will be compared to WLBU2 alone in order to determine whether addition of the CRAC motif enhances antiviral activity.

2.3 SPECIFIC AIM 3: TO ASSESS CYTOTOXICITY OF CRAC MOTIF CONTAINING PEPTIDES AGAINST A PANEL OF TRANSFORMED AND NON-TRANSFORMED CELLS AND CELL LINES.

To measure toxicity of peptides against host cells, two cytotoxicity assays will be carried out: hemolysis and MTS assays. These two measures of cytotoxicity were chosen because they are both established standards of the field and they measure cytotoxicity by different methods. The hemolysis assay measures direct lysis of red blood cells (RBCs) while the MTS assay measures metabolic activity of cells indicating viability. For the hemolysis assay, RBCs in phosphate buffered saline (PBS) will be treated with varying concentrations of each of the peptides to measure release of hemoglobin, indicating cell lysis. For the MTS assay, a panel of both transformed and non-transformed cells will be tested to determine a range of cytotoxic activity of the peptides. Transformed cells were chosen as they are the relevant indicator cells for each of the virus inactivation assays performed. A non-transformed cell line and primary cells were also chosen because previous research has found that transformed cells are more susceptible to peptide treatment than non-transformed cells. Cells will be treated with various concentrations of each peptide, and then allowed a short recovery period before carrying out the MTS assay for cell viability.

3.0 MATERIALS AND METHODS

3.1 MODELING

The peptide modeling program PEP-FOLD was used to predict the structure of CRAC motif-containing WLBU2 peptides (http://bioserv.rpbs.univ-paris-diderot.fr/PEP-FOLD/). Sequences were run on a short simulation and models were sorted by sOPEP, which clusters models based on similar energy states based on simplified side chains (74). PEP-FOLD predicts peptide conformations based on the amino acid sequence using coarse-grain simulation to look at interactions between four amino acids at a time (75). Models generated in PEP-FOLD are sorted into clusters based on structural similarity. All models that were analyzed were representative of a single model cluster. Models generated from PEP-FOLD were then analyzed using PyMol molecular visualization software version 0.99 (http://www.pymol.org/). Similarly, helical wheel projections and hydrophobicity predictions were created by HeliQuest (http://heliquest.ipmc.cnrs.fr/). Helical wheel projections were created using the α-helix setting to analyze the full amino acid sequence. This program then analyzes the physiochemical properties of the peptide based on its amino acid sequence and the forced helical conformation.

3.2 PEPTIDE SYNTHESIS

Amino acid sequences of the desired peptides (WLBU2 and CRAC modified versions) were produced by the University of Pittsburgh Peptide Synthesis Core of the Genomics and Proteomics Core Laboratories following previously reported synthesis and purification procedures optimized for WLBU2 production (76). Other stocks of the same peptides were produced commercially using similar methods by Genscript (Piscataway, NJ). All peptide preparations were purified by HPLC to at least 95% purity. Concentrations of peptide dissolved in sterile water were determined by a standard ninhydrin assay as previously reported (76). Concentrations were confirmed using spectrophotometric methods by A260/A280 determination on a NanoDrop 1000 spectrophotometer (NanoDrop, Wilmington, DE).

3.3 CIRCULAR DICHROISM SPECTROSCOPY

Measurements were taken at a 40 µM concentration of each peptide in the following solvent environments: deionized water, 6 mM sodium dodecyl sulfate (SDS), 30 mM SDS, and 30% tetrafluoroethylene (TFE). Circular dichroism (CD) measurements were taken with a Jasco spectrometer (Aviv Instruments, Lakewood, NJ) at room temperature with a 1 mm path length over 185 nm to 260 nm with machine units as output for five scans per sample. The mean residue ellipticities ([Θ]/1,000 × [(degree × square centimeters)/decimole]) were calculated of the averaged five scans using Dichroweb (http://dichroweb.cryst.bbk.ac.uk/) (77). These data were analyzed using the CDSSTR method (78; 79; 80) with SP175 as the reference data set (81). The CDSSTR method was chosen because it produces the most accurate analysis results and SP175

was chosen as the reference data set because it contains the most reference proteins at the necessary wavelengths for comparison to the data that was collected with CRAC motif containing peptides.

3.4 CELL PROPAGATION

The following cell lines were propagated in Dulbecco's Modified Eagle Medium (DMEM; Life Technologies, Grand Island,NY) containing 10% fetal bovine serum (FBS) and 1% L-glutamine: MDCK, MRC-5, HEK239T/17, VeroE6, and TZM-bl (NIH AIDS Research and Reference Reagent Program, Germantown MD) cells. To passage, cells were treated with 0.05% Trypsin/0.53 mM EDTA in HBSS (Corning, Manassas, VA) for 10-15 minutes before transferring a subset of cells to a new flask with fresh complete media.

3.5 ISOLATION OF HUMAN PERIPHERAL BLOOD MONONUCLEAR CELLS

Human PBMCs were isolated from heparinized human blood from healthy donors (with the approval of the University of Pittsburgh Institutional Review Board) as previously described (39). Briefly, Histopaque gradient centrifugation was performed at 1000 rpm for 20 min with the brake off. PBMCs were collected, washed with PBS at least twice, and suspended in PBS. Cells were stored in liquid nitrogen in 10% DMSO, 90% FBS for less than a month before use, with 80 – 85% viability maintained.

3.6 VIRUS STOCK PREPARATION

3.6.1 HIV

To produce stocks of HIV, HEK293T/17 cells plated in 6-well plates grown to 90 – 95% confluence were transfected with 2.5µg of DNA using Lipofectamine LTX and Plus reagent according to the manufacturer's instructions (Life Technologies, Grand Island NY). Infectious HIV-1 89.6 virus was produced by transient transfection of HEK293T/17 cells with the plasmid pUC19-89.6 wild type, with media replacement at 4 hours post transfection. Viral supernatant was retrieved 48 hours after the transfection and centrifuged at 663xg for 10 min at 4°C.

3.6.2 Influenza A

To produce stocks of influenza A, MDCK cells in a 150 cm^2 cell culture flask grown to about 90% confluence were infected with influenza virus strain PR8 (A/Puerto Rico/8/1934) at an MOI of 1. Infected cells were incubated in media containing DMEM, 0.2% Bovine Albumin Fraction V (BSA; Life Technologies, Grand Island,NY), and 2 ug/mL TPCK-treated Trypsin (Sigma-Aldrich, St. Louis, MO) for 48 hours until CPE was observed and cells were not adhered. Just before virus was collected, BSA was added to culture medium to a final concentration of 0.3%. Cells and culture supernatant were then centrifuged at 600xg for 10 min at 4°C to pellet debris. Virus was aliquoted and frozen before titration by plaque assay.

3.6.3 DENV

Stocks of DENV serotype 2 kindly provided by Priscila Castanha of Dr. Ernesto Marques's lab (Center for Vaccine Research, University of Pittsburgh).

3.7 ANTIVIRAL ACTIVITY

3.7.1 HIV

To test HIV inactivation, a viral infection neutralization assay was carried out on TZM-bl cells in 96-well flat bottom plates to measure production of luciferase under control of the HIV-1 promoter. Cells were plated at a concentration of 2.5×10^4 cells/well and allowed to adhere at $37^oC/5\%$ CO_2 for 7 hours. HIV strain 89.6 was diluted so as to produce about 3×10^4 RLUs/well in untreated control wells. Peptide dilutions were prepared in a 96-well U-bottom plate by 2-fold serial dilutions starting at 100 µM down to 0.78 µM in DMEM containing 10% FBS. Equal volumes of virus stock were added to each well of peptide for a final volume of 40 ul and incubated together at $37^oC/5\%$ CO_2 for 1 hour. Virus-peptide mixtures were then brought up to total volume of 200 ul (5 fold dilution) and plated on adhered TZM-bl cells for 1 hour and then removed and replaced with fresh complete media. Plates were incubated for 48 hours and then cells were lysed with 50µl of cell culture lysis reagent, and luciferase activity was read using the luciferase assay system according to the manufacturer's instructions (Promega, Madison WI) using an Orion Microplate Luminometer (Berthold, Oak Ridge TN).

3.7.2 Influenza A

To test influenza A inactivation, a plaque assay was carried out on MDCK cells (82) using virus that had been pre-incubated with peptide. Influenza strain PR8 was diluted to a final concentration of 160 pfu/ml then mixed with an equal volume of prepared dilutions of peptide. Peptide had been diluted by 2-fold serial dilution using DMEM containing 0.2% BSA in 1.5 mL Eppendorf tubes starting at 100 µM down to 0.78 µM. Peptide-virus mixtures were incubated at 37^{o}C/5% CO_2 for 1 hour. MDCK cells between passages 3 and 10 plated in 6-well plates at 8 x 10^5 cells/well were grown to 90-100% confluence were washed twice with serum-free media then exposed to pre-incubated virus-peptide mixtures for 45 minutes in duplicate. Virus and peptide were removed and replaced with plaquing media containing DMEM, 10% FBS, 2.5 ug/mL TPCK-treated Trypsin, and 0.4% agarose. Infected and treated cells were then grown at 37^{o}C/5% CO_2 for 5 days before being stained with 35% EtOH/0.25% Crystal violet overnight at 4^{o}C. Stain and agarose plugs were removed and plaques were counted by eye using a light box. All plaque assay experiments were carried out at least three times.

3.7.3 DENV

To test DENV inactivation, a plaque assay was carried out on VeroE6 cells (83) using serotype 2 virus that had been pre-incubated with various concentrations of peptide. Virus was diluted by 10^3 fold and mixed with an equal volume of prepared dilutions of peptide. Peptide had been diluted by 2-fold serial dilution using MEM containing penicillin/streptomycin, and Fungizone (Life Technologies, Grand Island NY) in a 96 well plate starting at 50 µM down to 1.5625 µM. Peptide-virus mixtures were incubated at 37^{o}C/5% CO_2 for 1 hour. VeroE6 cells

between passages 25 and 42 plated in 24-well plates at 1.5 x 10^5 cells/well 48 hrs in advance were grown to 90-100% confluence were then exposed to pre-incubated virus-peptide mixtures for 1 hr in duplicate. Virus and peptide were removed and replaced with semi-solid media containing 3% carboxymethylcellulose (CMC), MEM, 10% FBS, penicillin/streptomycin, and Fungizone. Infected and treated cells were then grown at 37^{o}C/5% CO_2 for 6 days before fixing and staining. Semi-solid medium was removed from cells before addition of formalin and cells were then allowed to incubate at room temperature for 1 hr. Formalin was removed, the cells were washed, and then crystal violet was added. Plates were incubated for 1 hr at room temperature and washed again before plaques were counted. All experiments were carried out at least three times.

3.8 CYTOTOXICITY

3.8.1 Red Blood Cell Lysis Assay

A modified version of the RBC lysis assay carried out by Deslouches et al. (39) was performed using RBCs collected during isolation of PBMCs. Erythrocytes were pelleted by centrifugation at 1000 rpm for 10 min then diluted to a 10% solution (1:10 dilution) in sterile phosphate buffered saline (PBS). Peptide dilutions were created in tissue culture-treated round bottom 96 well plates in duplicate ranging in concentration from 100 μM to 0.78 μM. Peptides were incubated at 37^{o}C/5% CO_2 for 1 hour before an equal volume of 10% RBCs were added to each well (1:2) dilution. To produce a standard curve for analysis, 0 to 50 μl of 5% RBC solution (1:20 dilution) was added to dH_2O to a final volume of 500 μl (up to 1:10 dilution) and incubated

for 1 hour along with peptide-RBC mixtures at 37°C/5% CO_2. These hemoglobin suspensions were then centrifuged at 600xg for 10 min to pellet intact RBCs. In a 96 well flat bottom plate, 20 ul of supernatant from each peptide-RBC mixture was diluted 10-fold in 180 ul of sterile dH_2O. Absorbance readings were taken at 570nm on a SpectraMax 340PC384 Absorbance Microplate Reader (Molecular Devices, Sunnyvale, CA).

3.8.2 MTS Assay

Cytotoxicity measurements were taken on selected transformed and non-transformed cells using a tetrazolium-based colorimetric MTS assay, a one-step variation of the classic MTT assay (84). The MTS assay measures cell viability by detecting metabolically active cells that reduce MTS to a colored formazan reagent. Cells were plated in 96-well plates and allowed to grow to 90 – 100% confluence. Peptides starting at 50 μM were diluted by serial two-fold in a 96 well U-bottom plate and incubated at 37°C/5% CO_2 for 1 hour. Cells were then treated with each concentration of peptides for 1 hour, at which time the peptide-containing supernatant was removed and replaced with fresh complete media. Cells were then allowed to recover at 37°C/5% CO_2 for 4 hours before performing an MTS assay. This assay was carried out using the CellTiter 96 AQueous One Solution Cell Proliferation Assay following the manufacturer's protocol (Promega, Madison, WI). Briefly, MTS reagent was added to cells, and then incubated at 37°C/5% CO_2 for 2 hours before spectrophotometric readings were taken at 490nm on a SpectraMax 340PC384 Absorbance Microplate Reader (Molecular Devices, Sunnyvale, CA).

4.0 RESULTS

4.1 DESIGN

4.1.1 CRAC Motif Design

Following the characteristic sequence (**L/V** – X(1-5) – **Y** – X(1-5) – **K/R**), CRAC motifs were designed for addition to WLBU2 to increase cholesterol specificity. Initially, addition of LWYIK from the HIV fusion protein gp41 was selected for evaluation because it is well-characterized (45; 46; 47) and would give us a basis of comparison for how a completely synthetically designed CRAC motif may function. In order to develop a CRAC motif with minimal amino acid differences from the sequence of WLBU2, a synthetically designed CRAC motif was created. The CRAC motif VWYVK was designed that follows the characteristic CRAC sequence as described above. This sequence is the shortest possible CRAC motif and minimizes differences between the WLBU2 amino acid sequence by only introducing two new amino acids, as opposed to four different amino acids found in LWYIK. By minimizing the number of unique amino acids in a sequence, the cost of production of peptides is reduced. While the CRAC sequence indicates it is possible to have an arginine in the last position, further minimizing amino acid differences, there is evidence that, in the case of the LWYIK motif, the

terminal lysine is important for maintaining structural flexibility of the peptide (43). For this reason, lysine was retained in the last amino acid position.

4.1.2 Predictive Modeling

Modeling was carried out in order to examine the predicted effect of CRAC motif contributions on WLBU2 structure and to determine the optimal location for this modification in the peptide sequence. These structural modeling studies employed PEP-FOLD modeling software, which has been optimized to predict secondary structure of short amino acid sequences based on a coarse grain, multiple simulation analysis using a structural alphabet for reference (75). In the models produced, we hoped to see that addition of the CRAC motif would not disrupt the predicted structure of WLBU2 and that the terminal CRAC motif would remain unstructured, thus maintaining the flexibility necessary for CRAC function (45). Each CRAC motif, LWYIK and VWYVK, was added to either the C- or N-terminus of WLBU2 and modeled using PEP-FOLD. PEP-FOLD sorts models into clusters that are ranked based on sOPEP scores. As described in Materials and Methods, sOPEP can score the models generated based on the energetic landscape of peptides with simplified side chains (74). Peptides with similar sOPEP scores are grouped together into clusters characterized by a single representative model. In C-terminal modeling, PEP-FOLD predicted 172 models sorted into five clusters for LWYIK and 190 models sorted into 8 clusters for VWYVK. For both motifs, a single model cluster each represented at least 95% of all the models generated (Figure 5a). These two largely representative models were then aligned to WLBU2 (Figure 5b). In all models generated, there was no predicted direct interaction between the CRAC motifs and WLBU2 peptide sequence. However, according to modeling predictions, addition of the CRAC motif to the C terminus of

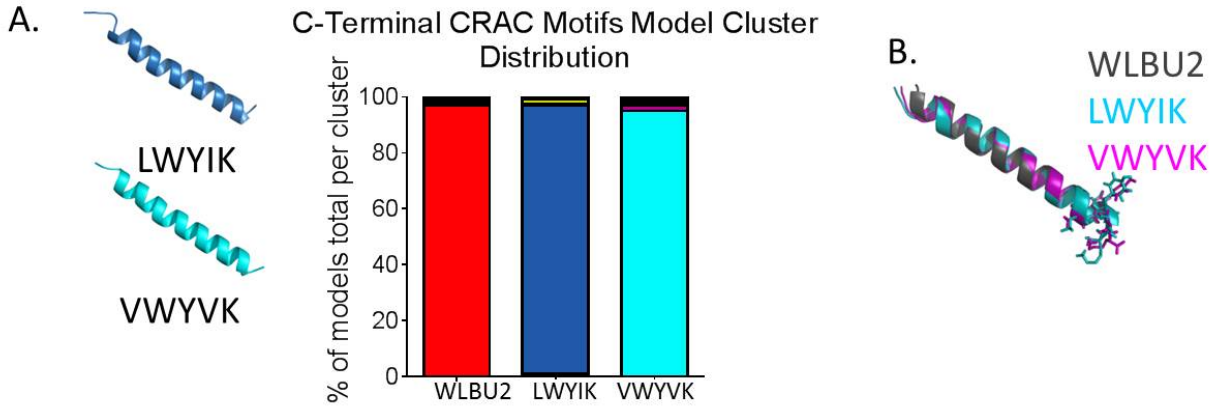

A. The most representative model clusters of WLBU2 containing each CRAC motif are shown on the left with cluser distributions shown on the right, where the colors of the models on the left correlate to the cluster distribution on the right. The models shown represent 95% of all models produced by PEP-FOLD. **B.** Alignment of models displayed in A with WLBU2. CRAC motif residues are represented by stick model to highlight the α-helical structure formed by the motif.

Figure 5. PEP-FOLD modeling predictions for WLBU2 peptides containing C-terminal CRAC motifs.

WLBU2 would have a largely helical structure maintained throughout the peptide, including the C-terminal CRAC motif. Because the C-terminal CRAC motif is helical, there is not the flexibility necessary for proper CRAC motif function.

In adding the CRAC motifs to the N-terminus of WLBU2, PEP-FOLD predicted 190 models sorted into 20 model clusters for LWYIK and 175 models sorted into 19 model clusters for VWYVK. None of the predicted models indicated any interaction between CRAC motifs and WLBU2 peptide sequence. Clusters containing the most models were selected for further analysis as they appeared to have lower sOPEP scores, indicating a more favorable energetic conformation. We found that for N-terminal LWYIK, three model clusters (3, 6, and 9) represented approximately 80% of all the models generated, while three model clusters of N-terminal VWYVK (1, 3, and 11) represented about 85% of all the models generated (Figure 6a).

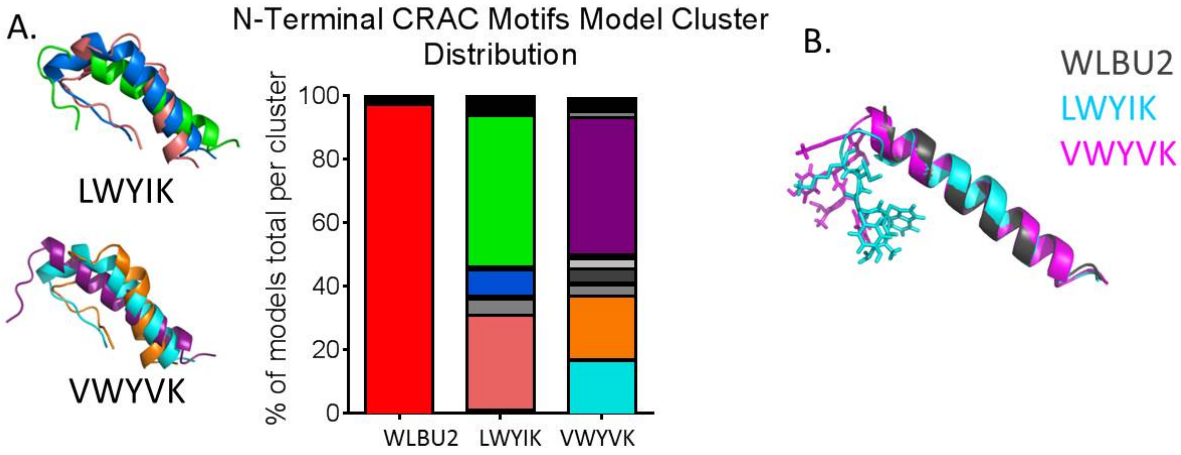

A. The most representative model clusters of WLBU2 containing each CRAC motif are shown on the left with cluster distributions shown on the right, where the colors of the models on the left correlate to the cluster distributions on the right. The models shown represent 80 - 85% of all models produced by PEP-FOLD. **B.** Alignment of a single model cluster displayed in A (LWYIK – green, cluster 9; VWYVK – aubergine, cluster 11) with unmodified WLBU2. CRAC motif residues are represented by stick model to highlight the predicted flexibility of the motif.

Figure 6. PEP-FOLD modeling predictions for WLBU2 peptides containing N-terminal CRAC motifs.

The largest cluster (3 for LWYIK and 11 for VWYVK) of these representative three were aligned to WLBU2 (Figure 6b). According to modeling predictions, addition of the CRAC motif to the N terminus of WLBU2 would produce a largely helical peptide with an unstructured N-terminal CRAC motif.

Based on the modeling predictions, four peptides containing each CRAC motif on the N-terminus either once or twice (as listed in Table 2) were selected for production by solid phase peptide synthesis (76). Peptides were produced with the CRAC motif added to the N-terminus twice to investigate whether addition of multiple CRAC motifs affects peptide activity or cholesterol specificity. Peptides containing two CRAC motifs were not modeled because at 34 residues long, PEP-FOLD software is less accurate in predicting secondary structure (75).

Table 2. CRAC Motif Containing Peptides.

Peptide	Length	Molecular Weight (g/mol)	Sequence
LWYIK	29	4104.04	LWYIKRRWVRRVRRWVRRVVRVVRRWVRR
LWYIK2	34	4807.93	LWYIKLWYIKRRWVRRVRRWVRRVVRVVRRWVRR
VWYVK	29	4075.99	VWYVKRRWVRRVRRWVRRVVRVVRRWVRR
VWYVK2	34	4751.82	VWYVKVWYVKRRWVRRVRRWVRRVVRVVRRWVRR

4.2 SECONDARY STRUCTURE CHARACTERIZATION

Once peptides had been produced, structural characterization was carried out by CD spectroscopy in the following solvent environments: dH_2O, 6 mM SDS, 30 mM SDS, and 30% TFE. TFE is a hydrophobic solvent that would mimic the hydrophobic core of a lipid bilayer, whereas SDS forms micelles acting as an approximate membrane mimic. SDS forms micelles at concentrations of 30% or greater at room temperature (85); micelles mimic the hydrophobic-aqueous interface that would be encountered at the surface of a lipid bilayer. Previous studies analyzing WLBU2 by CD spectroscopy indicated that WLBU2 assumes a predominantly random coil conformation with no appreciable structure in phosphate buffer (PB) which mimics an aqueous environment, whereas in 30% TFE, WLBU2 forms a distinct α-helix with approximately 81% helical content (35). For this study, mean residual ellipticity (MRE) values were calculated from machine units using the Dichroweb program and plotted versus wavelength. Predicted structural content for all peptides in each solvent environment is summarized in Table 3.

Table 3. Secondary structural content of CRAC motif containing peptides based on CD analysis using CDSSTR method on Dichroweb.

	dH_2O		6 mM SDS		30 mM SDS		30% TFE	
Peptide	α-Helix	Random Coil	α-Helix	Random Coil	α-Helix	Random Coil	α-Helix	Random Coil
LWYIK	55%	21%	85%	5%	88%	3%	78%	9%
LWYIK2	55%	21%	85%	4%	87%	4%	79%	6%
VWYVK	52%	23%	91%	2%	85%	3%	78%	9%
VWYVK2	56%	24%	88%	5%	82%	5%	76%	10%

For each of the CRAC motif containing peptides in dH_2O, MRE curves were typical of a random coil indicating that in water the peptides are in a random coil conformation with about 50% helical content (Figure 7a). In both 6 mM and 30 mM SDS, MRE curves revealed pronounced minima at 208 nm and 222 nm that are characteristic of peptides that are mostly α-helical in content (Figure 7b, c). In complexes with SDS, all CRAC motif containing peptides contained >80% helical character. Similar MRE curves were found when peptides were analyzed in the presence of 30% TFE (Figure 7d). In 30% TFE, all peptides were found to contain about 75% helicity. Based on CD spectroscopy, all of the CRAC motif containing peptides form similar structures to each other in each solvent environment and appear to characterize similarly to WLBU2 when compared to previously reported experiments. These findings are consistent with the modeling predictions showing that CRAC motif containing peptides maintain helical content.

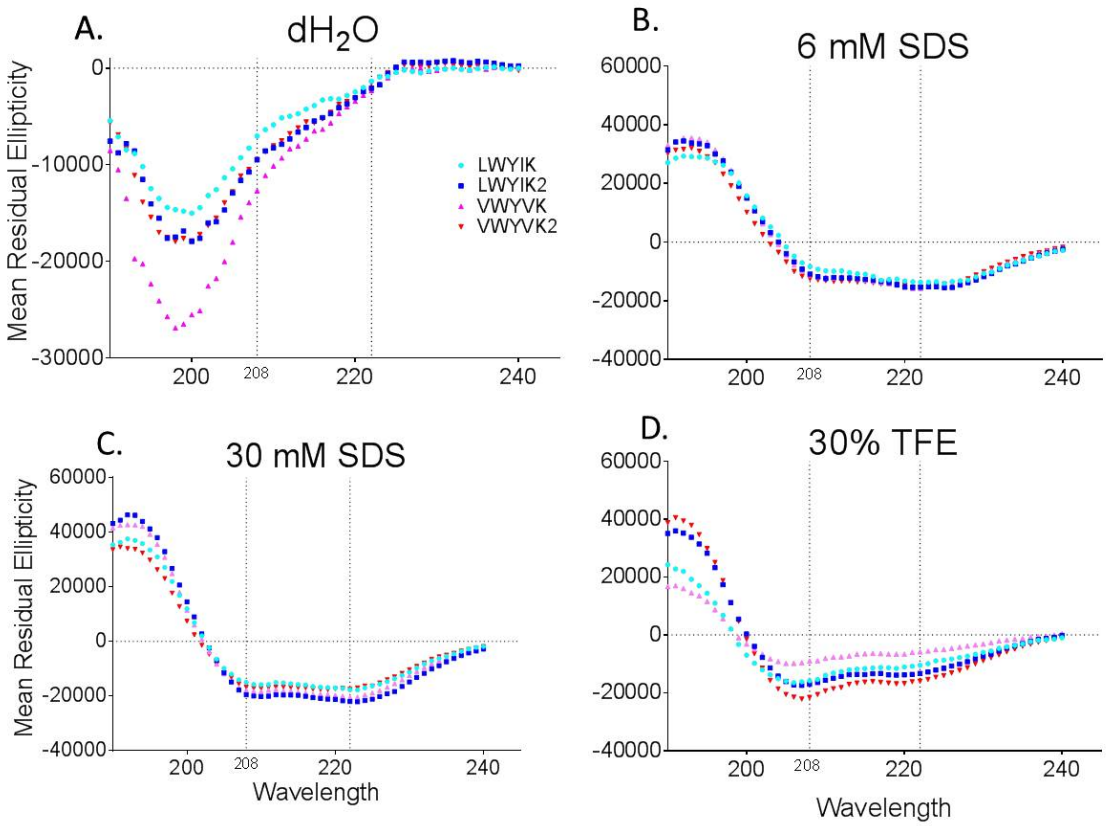

MRE ([Θ]/1,000 × [(degree × square centimeters)/decimole]) is plotted against wavelength. **A.** CD spectra in aqueous solvent - dH_2O. **B.** CD spectra in membrane mimic solvent - 6 mM SDS. **C.** CD Spectra in membrane mimic solvent - 30 mM SDS. **D.** CD spectra in hydrophobic solvent - 30% TFE.

Figure 7. CD spectroscopy results of CRAC motif containing peptides in various solvent environments.

4.3 ANTIVIRAL ACTIVITY

4.3.1 HIV

In order to determine antiviral activity of the various CRAC-modified peptides against HIV *in vitro*, viral inactivation was assessed by a luciferase-based infectivity assay system on

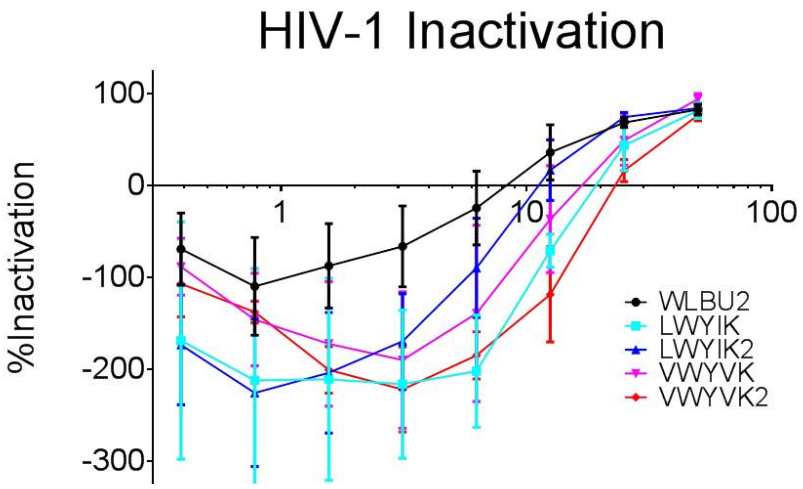

HIV-1 strain 89.6 was exposed to peptides serially diluted two-fold from 50 µM to 0.39 µM for 1 hr before exposure to TZM-bl cells. Infection was measured by detection of luciferase expression from the HIV-1 promoter. All peptides enhance infection at concentrations less than 12.5 µM, with greater enhancement observed for CRAC motif containing peptides. Experiments were repeated twice.

Figure 8. Percent inactivatin of HIV-1.

TZM-bl cells. HIV strain 89.6 was pretreated with varying concentrations of each of the peptides before exposure to TZM-bl cells. Percent inactivation was calculated based on comparison of luciferase production to untreated controls. For each of the peptides tested, viral inactivation was observed at the highest concentrations tested, 50 and 25 µM. However, at concentrations below 25 µM, all of the CRAC motif containing peptides showed enhancement of viral infection (Figure 8). This enhancement was greater than that observed for WLBU2, where WLBU2 still showed approximately 13% inactivation at 6.25 µM. At 6.25 µM, LWYIK and VWYVK2 enhanced infection by about 200% over untreated controls, whereas LWYIK2 and VWYVK enhanced infection by about 100% over untreated controls. While unmodified WLBU2 displayed enhancement of infection at concentrations below 6.25 µM, the effect was not as pronounced as with CRAC motif containing peptides.

4.3.2 Influenza A

In order to determine antiviral activity of the CRAC-modified peptides against influenza virus *in vitro*¸ inactivation was assessed by a standard plaque assay (82). Influenza A H1N1 strain PR8 was pretreated with varying concentrations of each of the peptides before exposure to MDCK cells. Percent plaque reduction was calculated based on comparison to untreated controls. All of the CRAC motif containing-peptides have similar activity against influenza as unmodified WLBU2 at concentrations lower than 6.25 µM (Figure 9). At concentrations greater than 6.25 µM, all peptides reduced plaques by about 90 - 100%. The data suggests that peptides that contain two CRAC motifs have enhanced antiviral activity as compared to corresponding peptides with only one CRAC motif. From these data, EC_{50} values were calculated for each of the peptides tested, as summarized in Table 4. The most active peptide LWYIK2 has at least twice the antiviral activity as WLBU2 with an EC_{50} value as low as 1.33 µM. Even at nanomolar concentrations, peptides with two CRAC motifs still retained antiviral activity. At 0.39 µM, LWYIK2 reduced plaques by about 31% while VWYVK2 reduced plaques by 37%, whereas at the same concentration WLBU2 has no activity against influenza A. These data indicate that pretreatment with CRAC motif-containing peptides enhances influenza virus inactivation as compared to WLBU2, with greatest activity displayed when two CRAC motifs are present.

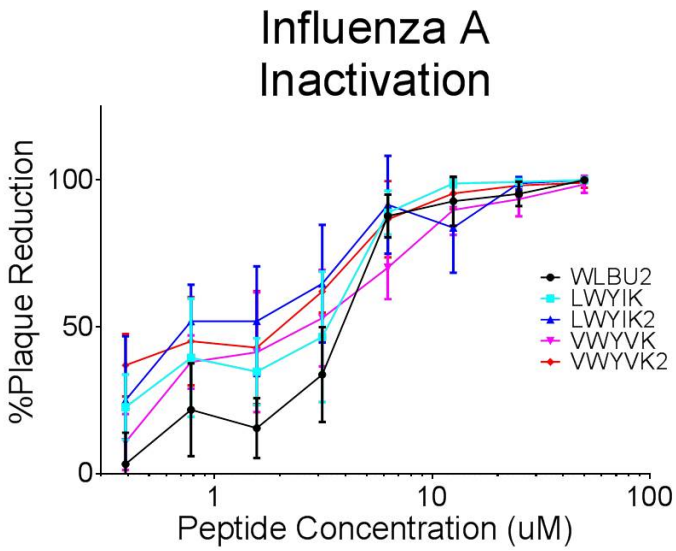

Influenza strain PR8 was exposed to peptides serially diluted two fold from 50 µM to 0.39 µM for 1 hr before exposure on MDCK cells. Percent plaque reduction was measured by comparison to untreated controls. CRAC motif containing peptides and unmodified WLBU2 display similar levels of antiviral activity. Experiments were repeated twice.

Figure 9. Percent plaque reduction of influenza A.

Table 4. Calculated EC_{50} of peptides against influenza A strain PR8.

Peptide	EC_{50} (µM)
WLBU2	**4.11± 1.08**
LWYIK	**4.23 ± 1.11**
LWYIK2	**1.33 ± 2.94**
VWYVK	**2.40 ± 1.56**
VWYVK2	**3.89 ± 1.15**

4.3.3 DENV

In order to determine antiviral activity of CRAC modified peptides against DENV *in vitro*¸ inactivation was assessed by a standard plaque assay (83). DENV serotype 2 was pretreated with varying concentrations of each of the test peptides before exposure to VeroE6 cells. Percent plaque reduction was calculated based on comparison to untreated controls. All of the test peptides inactivated DENV, and CRAC motif containing peptides outperformed unmodified WLBU2 alone (Figure 10). All of the CRAC motif containing peptides displayed almost 100% plaque reduction at concentrations as low as 1.56 µM. Even at 0.39 µM, the lowest concentration tested, CRAC motif containing peptides all displayed antiviral activity against

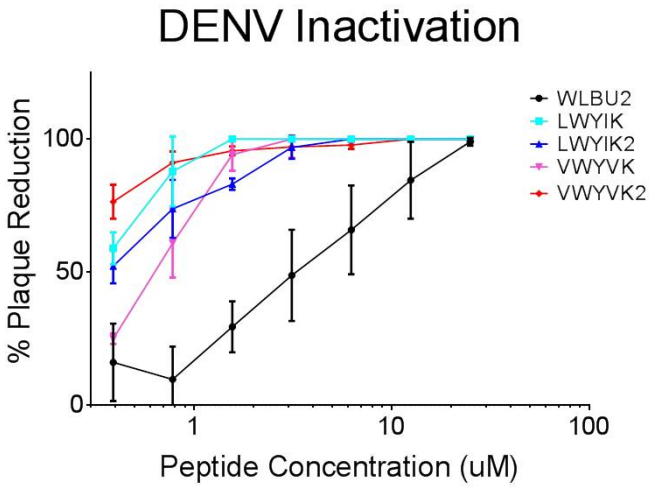

DENV serotype 2 was exposed to peptides serially diluted two fold from 50 µM to 0.39 µM for 1 hr before exposure on VeroE6 cells. Percent plaque reduction was measured by comparison to untreated controls. CRAC motif containing peptides LWYIK (cyan), LWYIK2 (blue), and VWYVK2 (red) were about 10-fold more antiviral than unmodified WLBU2. Experiments were repeated twice.

Figure 10. Percent plaque reduction of DENV.

DENV. At this concentration, WLBU2 reduced plaques by 16%, as compared to the most active peptide VWYVK2, which reduced plaques by 77%. Similarly, at 0.39 µM LWYIK and LWYIK2 reduced plaques by 59% and 52%, respectively. From these data, EC_{50} values were calculated for each of the peptides tested, as summarized in Table 5. EC_{50} values of LWYIK, LWYIK2, and VWYVK2 are about 10-fold lower than that of WLBU2 alone with 50% reduction of plaques observed at sub-micromolar concentrations. Taken together these data indicate that WLBU2 and CRAC motif containing peptides all inactivate DENV serotype 2 in a pretreatment assay.

Table 5. Calculated EC_{50} of peptides against DENV serotype 2.

Peptide	EC_{50} (µM)
WLBU2	**3.32 ± 0.64**
LWYIK	**0.340 ± 0.049**
LWYIK2	**0.366 ± 0.077**
VWYVK	**0.635 ± 0.053**
VWYVK2	**0.165 ± 0.055**

4.4 CYTOTOXICITY

4.4.1 Hemolytic Activity

To investigate the lytic effect of CRAC motif containing peptides against isolates of human RBCs, a hemolysis assay was carried out using a standard curve of water-treated RBCs

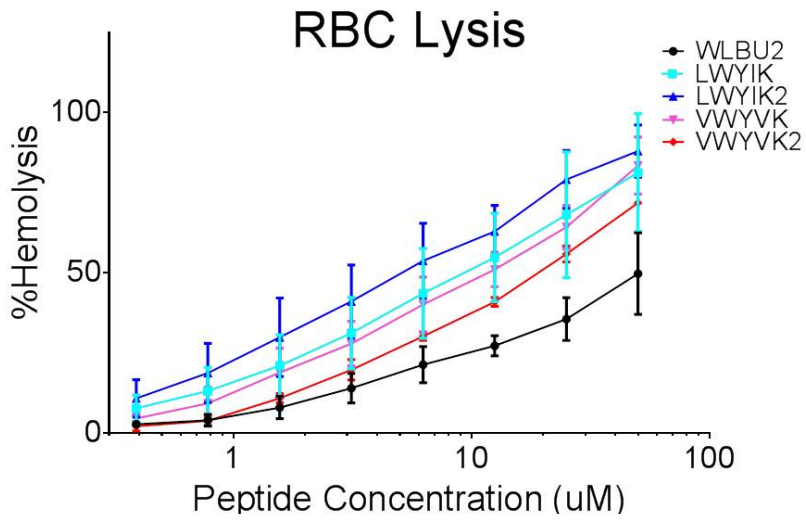

RBCs isolated from three independent donors were exposed to peptides two fold serially diluted from 50 µM to 0.39 µM for 1 hr. Hemolysis was measured by spectrophotometric analysis at 570 nm. CRAC motif containing peptides are all more hemolytic than unmodified WLBU2.

Figure 11. Percent hemolysis observed after peptide treatment.

for comparison (39). All RBCs were isolated by histopaque gradient centrifugation and resuspended in PBS containing no serum. This experiment was carried out individually three times with WLBU2 and each of the CRAC motif containing peptides using RBCs isolated from independent donors. As shown in Figure 11, the assays revealed very similar patterns of hemolysis among the different donor RBCs. In general, the CRAC motif containing peptides had greater hemolytic activity than unmodified WLBU. All CRAC motif containing peptides caused hemolysis of 50% of RBCs at concentrations less than 20 µM as summarized in Table 6. Unmodified WLBU2 displayed 50% hemolysis at a concentration approximately three times that as observed for CRAC motif containing peptides, indicating that addition of CRAC motifs enhances hemolytic activity of peptides. These data also indicate that peptides containing the CRAC motif LWYIK are about 2-fold more hemolytic than peptides that contain the VWYVK

motif. Furthermore, LWYIK2 is a more potent inducer of RBC lysis than LWYIK. On the other hand, VWYVK2 is less hemolytic than VWYVK. For all CRAC motif containing peptides, less than10% hemolysis was observed at concentrations less than 0.78 μM. These data indicate that all CRAC motif containing peptides are more hemolytic than unmodified WLBU2, with 50%

Table 6. Calculated 50% hemolysis values of RBCs treated with peptides.

Peptide	50% hemolysis (μM)
WLBU2	**40.16 ± 7.92**
LWYIK	**8.93 ± 2.25**
LWYIK2	**5.11 ± 0.92**
VWYVK	**10.50 ± 1.38**
VWYVK2	**17.98 ± 1.02**

hemolysis values varying based on CRAC motif sequence. Despite the increase in cytotoxicity, the concentrations at which CRAC motif containing peptides induce 50% hemolysis are still greater than the concentrations at which 50% virus inactivation is observed for both influenza A and DENV, indicating that therapeutic levels of peptides are much lower than those at which hemolysis occurs. For all of the peptides, EC_{50} values against DENV are at least 12 fold lower than 50% hemolytic values, and in the case of VWYVK2, the EC_{50} value is over 100 fold lower than the 50% hemolytic concentration.

4.4.2 MTS Assay

MTS assays were carried out on a panel of transformed and non-transformed cells to assay the effects of peptide treatment on cell viability. The MTS assay measures the amount of MTS that is reduced to a colored formazan product by metabolically active cells as a measure of viability (86). Cells were treated with various concentrations of each peptide, and then allowed a four hour recovery period in fresh complete media before cell viability measurements were taken. A four hour recovery period was chosen to allow cells a chance to respond to peptide treatment without allowing measurable cell growth over baseline before treatment. Two transformed cell lines, TZM-bl and MDCK cells, were chosen to be analyzed as they are the relevant indicator cells used for the HIV and influenza A viral inactivation assays, respectively. The human fetal foreskin fibroblast cell line, MRC-5, was chosen because the cells are non-transformed (87) and had been considered in the past for use in production of influenza vaccines (88). PBMCs were tested because they are non-transformed, primary cells that WLBU2 had previously been tested against in a similar MTT assay (39). Both transformed and non-transformed cells were tested for cytotoxicity because previous studies have shown that some AMPs are more cytotoxic on transformed cells than on primary or non-transformed cells (89; 90; 91).

Figure 12 shows viability of the various cells treated with concentrations of each of the peptides ranging from 50 µM to 0.39 µM. The cytotoxicity levels are expressed as a percentage of cell viability compared to untreated controls. Table 7 lists 50% cytotoxic concentrations (CC_{50}), defined as the concentration at which there is a 50% reduction in cell viability as compared to an untreated control, for each of the peptides against each of the cells tested. For all the cells tested, CRAC motif containing peptides displayed similar cytotoxicity to WLBU2. For

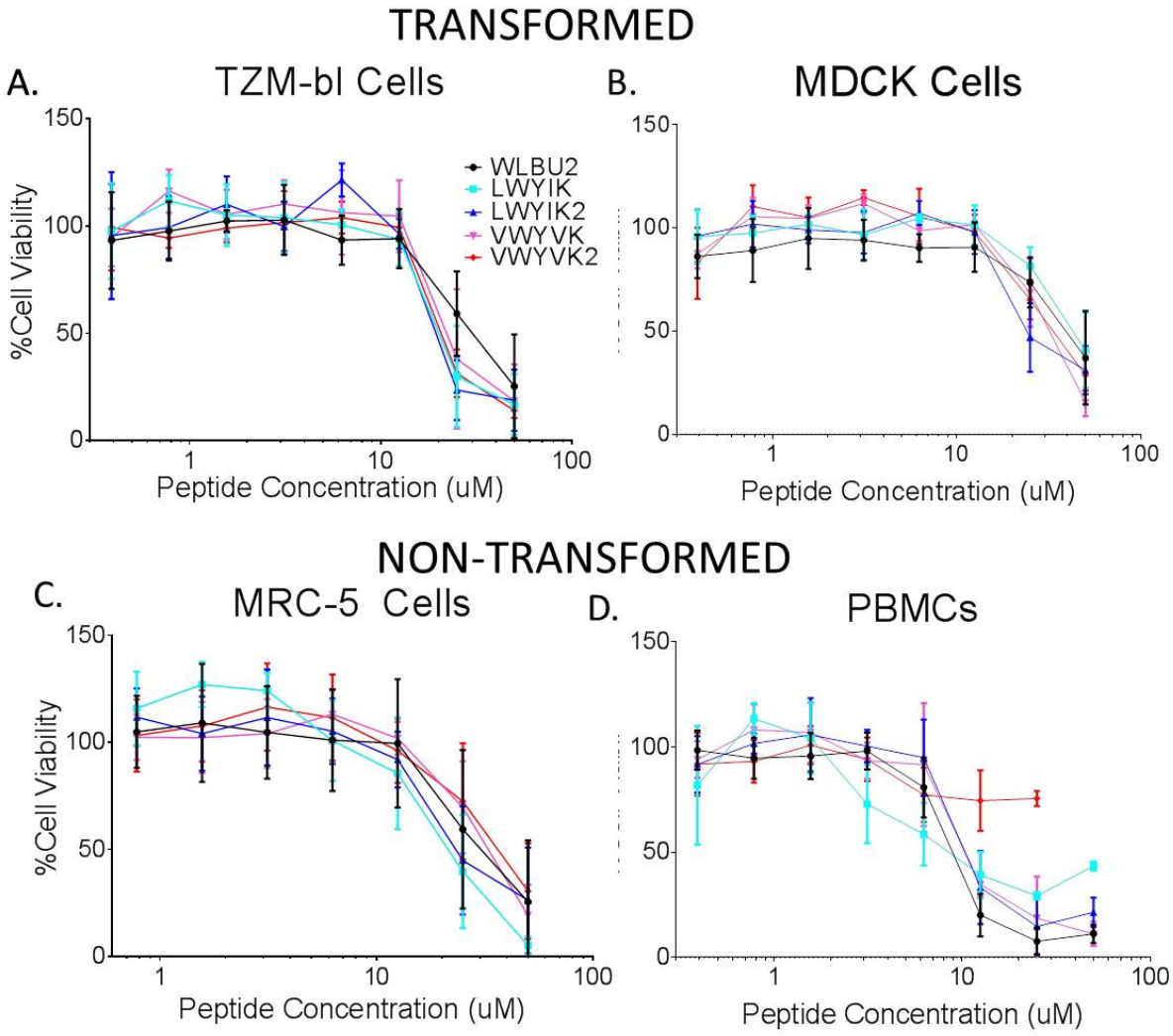

Cells were exposed to two fold serially diluted peptide ranging in concentration from 50 µM to 0.39 µM for 1 hr. Peptides were removed and cells were allowed to recover in fresh complete media for 4 hrs before remaining cell viability was read by MTS assay. Top row shows peptide cytotoxicity on transformed cell lines TZM-bl (**A.**) and MDCK (**B.**), the relevant indicator cells for HIV and influenza A infectivity assays, respectively. Bottom row shows peptide cytotoxicity on non-transformed cells MRC-5 cells (**C.**) and PBMCs (**D.**) Experiments were repeated three times.

Figure 12. Cell cytoxocity as measured by MTS assay.

the cell lines tested (TZM-bl, MDCK, and MRC-5), there is little to no difference in cytotoxicity observed on transformed versus non-transformed cell lines. CC_{50} values against each of the cell lines tested are significantly higher than the EC_{50} values calculated against influenza A and DENV, indicating that therapeutic levels of peptides are much lower than concentrations at which these peptides are causing cytotoxicity. For all of the peptides tested, CC_{50} values were 10 to 30-fold higher than the EC_{50} values against influenza A, and as great as 200-fold higher than the EC_{50} values against DENV.

Table 7. Calculated CC_{50} values (μM) from MTS assay for each of the peptides against all of the cells tested.

	TRANSFORMED		NON-TRANSFORMED	
Peptide	**TZM-bl**	**MDCK**	**MRC-5**	**PBMC**
WLBU2	30.64 ± 4.89	39.58 ± 8.36	31.21 ± 6.70	8.96 ± 0.79
LWYIK	21.14 ± 2.65	43.53 ± 4.72	21.93 ± 3.51	10.25 ± 3.72
LWYIK2	20.65 ± 3.70	29.09 ± 4.20	26.53 ± 4.55	10.95 ± 1.38
VWYVK	23.25 ± 2.97	31.19 ± 2.90	32.43 ± 3.57	11.24 ± 1.72
VWYVK2	22.01 ± 2.25	33.85 ± 4.97	36.53 ± 6.46	N/A

Primary, non-transformed PBMCs were isolated from individual donors and stored in liquid nitrogen. Cell stocks were then thawed and resuspended in serum-containing media before each MTS assay was performed. PBMCs were the most susceptible to peptide treatment of all of the cells tested with CC_{50} values three fold lower than that observed on the cell lines tested. Additionally, WLBU2 appeared to be more cytotoxic than CRAC motif containing peptides. For the peptide VWYVK2, data were omitted at the highest concentration tested due to issues with

solubility. Spectrophotometric readings taken for VWYVK2 at 50 µM and 25 µM showed greater absorbance values due to insolubility of the peptide at those concentrations. Higher absorbance values indicate greater cell viability in the MTS assay, whereas for VWYVK2 greater absorbance values were likely a factor of peptide solubility. For all other peptides, at the highest concentrations tested, peptides were soluble and the spectrophotometric readings were consistent with cell viability readings on the other cell lines tested by MTS assay, where cells treated with higher concentrations of peptides displayed less cell viability.

Selective indices were calculated using CC_{50} values obtained from MDCK cells and EC_{50} values that were reported above for influenza A and DENV. These values are listed in Table 8.

Table 8. Selective indices of peptides comparing CC_{50} of MDCK cells to EC_{50} against influenza A and DENV.

Peptide	Influenza A	DENV
WLBU2	7.45	9.23
LWYIK	5.00	62.2
LWYIK2	15.5	56.4
VWYVK	9.69	36.6
VWYVK2	5.66	133

For influenza A, selective indices for WLBU2 and most CRAC motif containing peptides were similar with values ranging from 5 to 9. In the case of LWYIK2, the selective index was 2-fold higher than the selective index for unmodified WLBU2 indicating that the peptide has similar cytotoxic affect, with greater antiviral activity. For DENV, selective indices of CRAC motif containing peptides were 3- to 15-fold higher than that of unmodified WLBU2. For the peptide VWYVK2, the selective index with 133 indicating that the concentration at which peptide causes

cytotoxicity is 133 times the concentration at which peptide displays antiviral activity. The selective indices for DENV indicate that CRAC motif containing peptides have greater antiviral activity than unmodified WLBU2.

5.0 DISCUSSION

While AMPs have been extensively explored for their potential as antibiotic alternatives, little work has been done to design peptides to specifically enhance antiviral properties. To date there is only a limited number of antiviral drug treatments available and these are always virus specific. The use of membrane-disruptive peptides as antiviral therapy is an attractive goal because treatment could be used against a variety of viral diseases that affect populations globally. Preliminary observations using the engineered AMP WLBU2 indicated antiviral activity against multiple enveloped viruses suggesting its potential as a broad spectrum antiviral treatment. However, viral envelope lipids lack the high concentration of negative charge that is the basis of AMP interaction with and inactivation of bacterial membranes. While viral envelopes are not highly negatively charged, mammalian viral envelopes do contain relatively high levels of cholesterol compared to their target cells, presumably due to virus budding at cellular lipid rafts. Thus, we hypothesized that the addition of CRAC motifs to WLBU2 could substantially increase binding to viral envelope lipids and increase viral inactivation. The current studies demonstrate that the addition of CRAC motifs to the N-terminus of WLBU2 yielded only a modest 2-fold increase in antiviral activity of WLBU2 against influenza A , with about a 10-fold increase in antiviral activity against DENV. This increase in antiviral activity was accompanied by a 3-fold increase in the levels of hemolysis and no change in cell viability as

compared to unmodified WLBU2 as measured by MTS assay *in vitro*, the therapeutic index of WLBU2 and CRAC-modified derivatives remained similar.

Initial modeling studies were carried out to predict how addition of a CRAC motif to WLBU2 could affect secondary structure. PEP-FOLD modeling predictions indicated that addition of the CRAC motif to the N-terminus of WLBU2 would be preferred over C-terminal addition because the CRAC motif had no predicted structure, and the main helix of WLBU2 was mostly undisturbed. Peptides produced by solid phase peptide synthesis were characterized by CD spectroscopy. In agreement with PEP-FOLD modeling predictions, CRAC motif containing peptides had >70% helicity and ≤10% random coil in hydrophobic environments (SDS and TFE) according to secondary structure analysis using CD data. Furthermore, in dH_2O, peptides contained about 5-fold more random coil structure. Based on previously reported data, the secondary structures of N-terminal CRAC motif containing WLBU2 peptides does not appear to differ significantly from WLBU2 alone in the same solvent environments. This suggests that addition of the CRAC motif does not disrupt the secondary structure previously observed with WLBU2. These data also suggest that PEP-FOLD modeling predictions based on lowest energy conformations agree with empirical secondary structure characterizations of peptides in hydrophobic environments.

CRAC motif containing peptides were tested against a panel of viruses representing different envelopes with diverse lipid to envelope protein compositions. Viruses were selected based on the protein content found on the envelope surface. All of the viruses tested, HIV, influenza A, and DENV, have membranes that are enriched for cholesterol. Other studies have shown that for each of these viruses, cholesterol is necessary for proper infection as without the incorporation of cholesterol there is impaired infection. The viral envelope of HIV contains only

about 20 trimers of envelope protein resulting in a very low protein-to-lipid ratio and high exposure of lipid at the surface of the virion. Influenza A has an intermediate protein-to-lipid ratio with a more dense membrane surface covering of HA and NA proteins. DENV has a very high protein-to-lipid ratio, with an outer proteinaceous layer covering the membrane, allowing very little surface lipid exposure. Based on these properties, this panel of viruses represents a gradient of membrane protein content and lipid surface exposure to test the range of antiviral activity of peptides. This panel of reference viruses allowed us to assess the effects of lipid exposure on peptide efficacy.

Unexpectedly, WLBU2 and the CRAC motif containing peptides all displayed enhancement of HIV infection in a pretreatment assay. We found that CRAC motif containing peptides were greater enhancers of infection than WLBU2 alone, showing up to a 200% increase in infection for the cases of LWYIK and VWYVK2. For CRAC motif containing peptides, this enhancement effect was observed at concentrations less than or equal to 12.5 µM. WLBU2 alone displayed enhancement of infection at concentrations less than or equal to 3.1 µM, with less of an increase of infection observed than for any of the CRAC motif containing peptides. For all of the peptides, inactivation of HIV was only observed at concentrations greater than 12.5 µM for each of the peptides tested. However, because these peptides show greater cytotoxicity at these concentrations, it is likely that what is observed as inactivation could be caused by toxic effects of the peptides directly on the cells.

These results were surprising because the surface of the HIV virion is sparsely populated by Env proteins with a high lipid surface exposure. We hypothesized that this high level of lipid surface exposure would make viruses more susceptible to antiviral treatment as peptides would readily be able to access the membrane for disruption, leading to inactivation. In contrast to this

prediction, peptide treatment of HIV led to enhancement of infection. The mechanism leading to this enhancement phenomenon is uncertain. HIV infection is more efficient when the viral envelope has a greater fluidity (92). Peptide interactions with the viral envelope may not disrupt the membrane fully, but perhaps increase the fluidity enough to enhance the efficiency of infection. CRAC motif containing peptides would enhance infection more as they would be expected to interact more readily with the cholesterol-rich viral envelope than WLBU2 alone. Another possible hypothesis for this enhancement effect is based on previous observations of a semen protein called semen-derived enhancer of viral infection (SEVI) (93). It has been shown that the cationic properties of SEVI alone are enough to act as a polycationic bridge to neutralize repulsion effects between a negatively charged virion and a target cell (94). Because WLBU2 and the CRAC motif containing peptides are highly cationic, it's possible that we are observing a similar effect in which these AMPs enhance HIV infection by increasing interactions between virions and target cells. In this model, CRAC motif containing peptides are better enhancers of infection because they are slightly more negative increasing the interaction between peptides and virus, while the overall highly cationic charge of the peptides could create the polycationic bridges proposed to enhance infection.

In marked contrast to HIV, WLBU2 and all of the CRAC motif containing peptides inactivated influenza virus *in vitro* with EC_{50} values of about 1 – 4 μM. All of the CRAC motif containing peptides showed similar activity to unmodified WLBU2 with EC_{50} values less than approximately 4 μM. CRAC motif containing peptides were marginally better at inactivating influenza A, whereas the peptide LWYIK2 was the most active with an EC_{50} value of 1.33 μM. It is unclear from this data whether LWYIK or VWYVK confers greater cholesterol specificity, or whether the addition of two CRAC motifs enhances this specificity. Cytotoxicity is an issue with

this experiment as well because significant reduction in cell viability was observed at concentrations greater than or equal to 25 μM. At the highest concentrations tested, it is unclear whether the peptide is blocking infection or killing cells that would become infected with live and active virus. Despite this concern, based on the MTS assay, there was no observable cytotoxicity on cells at concentrations less than or equal to 12.5 μM, while at this same concentration at least 75% viral inactivation was observed for all of the peptides. Furthermore, the therapeutic index between the EC_{50} and CC_{50} values is similar between the CRAC motif containing peptides and unmodified WLBU2. These data suggest that therapeutic concentrations of peptide are much less than the concentrations required to cause significant cytotoxic effect. Further studies on the mechanism of action of these peptides are required, such as flow cytometry experiments that analyze infection and cell apoptotic state concurrently after peptide exposure.

Based on the levels of surface exposure of envelope lipids, we predicted that DENV would be the least sensitive to inactivation by WLBU2 and its CRAC-modified derivatives. Contrary to this hypothesis, we observed that DENV was the most sensitive to inactivation by the engineered antimicrobial peptides. This observation suggests that there may be other mechanisms of virus inactivation in addition to lipid disruption. One possible mechanism of action is by peptide blocking cell surface receptors. The cellular receptors of influenza A and DENV, sialic acid (95) and heparan sulfate (96), respectively, are both negatively charged molecules found on the cell surface. Because these peptides are highly cationic, introduction of these peptides during infection may block viral entry by peptide binding to cell surface receptors, blocking interactions between viruses and their necessary receptors. Further studies on

the mechanism of action are required, including confocal microscopy studies using fluorescently tagged peptides to see whether peptide colocalize with necessary receptors for viral entry.

Differences in viral inactivation observed may also be due to the types of *in vitro* experiments used. While both the influenza A and DENV assays used a standard plaque assay to measure virus inactivation, the HIV infectivity assay uses an indicator cell system as a secondary measure of infection. One potential problem with this difference in techniques is that it makes comparison between viruses difficult as the *in vitro* assays are not directly comparable. Furthermore, biological differences between each of the viruses tested may also account for some of the variability in activity. Depending on how the virus is grown, HIV produces as few as 60,000 particles per infectious unit (97), whereas influenza produces an average of 40 particles per plaque forming units (PFU) (98) and DENV produces about 1,500 particles per PFU (99). In infectivity assays where there are many more non-infectious particles present, as is the case with HIV, it is possible that treatment peptides present are less effective since they would also be exerting any membrane disruptive effects on non-infectious particles as well as infectious particles. If there are vastly more non-infectious particles present, peptides would be less likely to encounter infectious particles. These differences in viral production efficiency may account for some of the differences observed in antiviral activity.

One concern in designing and testing all new antimicrobial therapies is the potential cytotoxic effect the treatment could have against mammalian host cells. We measured the cytotoxic effect of our peptides using two different methods that are both standard in the field. First, the hemolytic effect of WLBU2 and CRAC motif containing peptides was tested in a RBC lysis assay to measure release of hemoglobin from peptide treated cells. All CRAC motif containing peptides were approximately 3-fold more hemolytic than WLBU2 alone. This assay

was carried out on RBCs that had been isolated from donors and resuspended in PBS. However, in an *in vivo* system, RBCs would be in a more complex environment containing serum. Experiments have shown that AMPs have dampened cytotoxic activity in serum and whole blood environments and previous experiments with WLBU2 showed little peptide-induced cytotoxicity in whole blood (39). To determine whether serum alters cytotoxic activity of peptides, hemolysis assays could be carried out in the presence of serum or in whole blood, as done previously with WLBU2.

CRAC motif containing peptides may be more cytolytic to RBCs because erythrocytes have been shown to have increased average cholesterol content in the lipid membrane as compared to other human cells (100). Thus, peptides containing a cholesterol targeting sequence would likely increase cytolytic effect on RBCs. While all blood was taken and isolated from healthy donors, cholesterol content of erythrocytes has been shown to be intimately linked to disease state (101; 102) and is sensitive to changes in plasma cholesterol levels (103). Cytolytic effects of CRAC motif containing peptides may not be as pronounced on other mammalian cells where the cholesterol content of the membrane is lower and less sensitive to circulating cholesterol levels.

Cytotoxicity was also measured by MTS assay which detects oxidative processes in mitochondria reflected in color change by tetrazolium reduction to a formazan product that only occurs in metabolically active and therefore viable cells. This is a standard assay often used to measure cell viability, proliferation, or cytotoxicity (104). We tested a panel of cells and cell lines that included two transformed cell lines, a non-transformed cell line, and primary, non-transformed cell isolates. Some increase in cytotoxicity was expected, as mammalian cells have regions of the membrane that are enriched for the cholesterol and could possibly attract CRAC

motif containing peptides. For all of the cell lines tested, CRAC motif containing peptides and WLBU2 displayed similar levels of cytotoxicity, with CC_{50} values of approximately 30 μM. Furthermore, we did not detect any significant differences between cytotoxicity observed on non-transformed and transformed cell lines. Overall, the data indicate that the addition of either CRAC motif to WLBU2 does not chance the cytotoxicity of peptides based on MTS assay.

Previous research has shown that transformed and cancer cells are more susceptible to treatment with AMPs. Comparison of CC_{50} values between the transformed and non-transformed cell lines tested (TZM-bl, MDCK, and MRC-5) reveals no significant difference in cytotoxicity, contrary to what was expected. Surprisingly, PBMCs had the lowest CC_{50} values averaging about 10 μM, indicating that they were most susceptible to peptide treatment. Because these are primary isolates that are not an expanding population, it's possible that they have inherently lower metabolic activity. Indeed, absorbance values for PBMCs in the MTS assay were always lower than those measured for all other cells tested following all of the same assay conditions. This highlights the limitations of the MTS assay as it does not directly measure the live/dead state of a cell, but rather whether it is metabolically active. This indirect measure of cell viability may not be ideal for determining direct killing of cells. Peptides may interfere with the ability of the tetrazoilium dye to enter cells for reduction, or there may be a direct interaction between components of the reduction pathway and peptides. Multiple other measures of cytotoxicity are possible that would help determine whether peptides induce direct killing of cells. Simple live/dead staining, detected by flow cytometry, may be a better way to detect cell death as the live/dead stain directly measures live cells versus dead cells on a cell by cell basis.

These data indicate important properties of the CRAC motif sequence itself. Based on the antiviral activity and cytotoxicity data, both the LWYIK and VWYVK CRAC motifs behave

similarly to one another. This indicates that CRAC motifs can be designed synthetically with similar levels of activity to naturally occurring sequences. The results also show that addition of two CRAC motifs to WLBU2 does not alter activity as compared to peptides with only one CRAC motif, indicating that there is no additive effect with multiple CRAC motifs in the context of short peptide sequences. These data indicate that addition of the CRAC motif only slightly alters cytotoxicity, whereas peptides containing CRAC motifs are slightly more cytotoxic than WLBU2 alone. This is not necessarily surprising considering that mammalian cells are known to have regions of the membrane enriched for cholesterol that could attract CRAC motif containing peptides, leading to membrane disruption.

These data, taken together, have important implications in AMP design. The pattern of antiviral activity observed with these peptides against the chosen panel of viruses indicates that the mechanism of action of AMPs against mammalian viruses may not be dependent on lipid exposure as currently presumed. We expected that addition of the CRAC motif would direct peptides to cholesterol rich viral envelopes and disrupt the membrane thereby inactivating virus. Viruses with greater surface lipid exposure should be more susceptible to peptide treatment based on this mechanism because peptides would have easier access to the envelope. Contrary to this hypothesis, our results indicate that viruses with less lipid surface exposure are more susceptible to peptide treatment. These results are interesting because they suggest that there is a different mechanism of antiviral activity of these peptides. Establishing what this mechanism is will be important in developing other peptides with greater antiviral activity, discovering whether viruses could develop resistance, and determining other viruses against which these peptides would be effective.

This work represents a novel approach to developing antiviral therapeutics by targeting a property of viral envelopes shared between many different virus families. This work indicates that addition of the CRAC motif to the N-terminus of WLBU2 does not significantly affect the antiviral activity of this peptide in some cases. In the case of HIV, addition of the CRAC motif to WLBU2 caused a greater enhancement of infection than that observed with WLBU2 alone. In the case of influenza A, addition of the CRAC motif did not significantly affect antiviral activity as compared to WLBU2. When peptides were tested against DENV, CRAC motif containing peptides were at least five fold more effective at blocking DENV infection than WLBU2 alone, with activity observed at sub-micromolar concentrations. We found that cytotoxicity of CRAC motif containing peptides was not significantly different from that WLBU2 when compared to a panel of transformed and non-transformed cells and cell lines by MTS assay. Further studies should be conducted to determine both the range of antiviral activity of WLBU2 and CRAC motif containing peptides as well as the mechanism of action.

6.0 PUBLIC HEALTH SIGNIFICANCE

Viral diseases, including HIV, influenza, and DENV, are significant contributors to global disease burden. However, for most viral disease, no antiviral disease treatment exists. For the antiviral therapeutics that do exist, treatment is virus-specific. This work represents a novel antiviral strategy by targeting a characteristic shared between enveloped mammalian viruses. The goal of this work was to create a broadly active antiviral peptide that could be used to treat viral disease caused by enveloped viruses. Targeting the viral envelope for disruption is an attractive concept because resistance mechanisms would be extremely difficult to develop naturally. Further studies of the mechanism of action of CRAC motif containing peptides could allow development of peptides with even greater antiviral activity and reduced cytotoxicity. Antiviral therapies that could be used to treat multiple viral infections would significantly impact public health by reducing the burden of disease caused by enveloped viruses.

BIBLIOGRAPHY

1. *Antimicrobial Peptides of Multicellular Organisms.* **Zasloff, Michael.** 6870, s.l. : Nature, 2002, Vol. 415.
2. *The role of antimicrobial peptides in animal defenses.* **Hancock, Robert E.W and Scott, Monisha G.** 16, 2000, PNAS, Vol. 97, pp. 8856-61.
3. *Mechanisms of Antimicrobial Peptide Action and Resistance.* **Yeaman, Michael R and Yount, Nannett Y.** 1, 2003, Pharamacological Reviews, Vol. 55, pp. 27-55.
4. *The Antimicrobial Peptide Database.* [Online] University of Nebraska Medical Center Department of Pathology & Microbiology. [Cited:] http://aps.unmc.edu/AP/main.php.
5. *Cationic Peptides: A New Source of Antibiotics.* **Hancock, Robert EW and Lehrer, Robert.** 2, 1998, Trends in Biotechnology, Vol. 16, pp. 82-88.
6. *Antimicrobial Peptides: Primeval Moleculars or Future Drugs?* **Peters, Brian M, Shirtliff, Mark E and Jabra-Rizk, Mary Ann.** 10, 2010, PLoS Pathogens, Vol. 6.
7. *Emerging Themes and Therapeutic Prospects for Anti-Infective Peptides.* **Yount, Nannett Y and Yeaman, Michael R.** 2012, Annual Review of Pharamacologyl Toxicology, Vol. 52, pp. 337-60.
8. *Human Defensins and LL-37 in Mucosal Immunity.* **Doss, Mona, et al., et al.** 1, 2010, Journal of Leukocyte Biology, Vol. 87, pp. 79-92.
9. *Defensins: Antimicrobial Peptides of Innate Immunity.* **Ganz, Tomas.** 9, 2003, Nature Reviews Immunology, Vol. 3, pp. 710-20.
10. *The Mechanism of Action of Antimicrobial Peptides: Lipid Vesicles vs. Bacteria.* **Melo, Manuel N and Castanho, Miguel ARB.** 2012, Frontiers in Immunology, Vol. 3.
11. *From "Carpet" Mechanism to de-novo Designed Diastereomeric Cell-Selective Antimicrobial Peptides.* **Shai, Yechiel and Oren, Ziv.** 10, 2001, Peptides, Vol. 22, pp. 1629-41.
12. *Diversity of Antimicrobial Peptides and Their Mechanisms of Action.* **Epand, Richard M and Vogel, Hans J.** 1-2, s.l. : Biochimica et Biophysica Acta - Biomembranes, 1999, Vol. 1462.
13. *Cationic Antimicrobial Peptides as Novel Cytotoxic Agents for Cancer Treatment.* **Mader, Jamie S and Hoskin, David W.** 8, 2006, Expert Opinion on Investigational Drugs, Vol. 15, pp. 933-46.
14. *Studies on Anticancer Activities of Antimicrobial Peptides.* **Hoskin, David W and Ramamoorthy, Ayyalusamy.** 2, 2008, Biochimica et Biophysica Acta, Vol. 1778, pp. 357-75.
15. *A Novel Granulocyte-Derived Peptide with Lipopolysaccharide-Neutralizing Activity.* **Larrick, James W, et al., et al.** 1, 1993, Journal of Immunology, Vol. 152, pp. 231-40.

16. *High-Quality 3D Structures Shine Light on the Anitbacterial, Anti-Biofilm, and Antiviral Activities of Human Cathelicidin LL-37 and its Fragments.* **Wang, Guangshun, et al., et al.** 2014, Biochimica et Biophysica Acta.
17. *Human Cathelicidin, hCAP-18, is Processed to the Antimicrobial Peptide LL-37 by Extracellular Cleavage with Proteinase 3.* **Sorensen, Ole E, et al., et al.** 12, 2001, Blood, Vol. 97, pp. 3951-59.
18. *Antiviral Activity and Increased Host Defense Against Influenza Infection Elicited by the Human Cathelicidin LL-37.* **Barlow, Peter G, et al., et al.** 10, 2011, PLoS One, Vol. 6.
19. *Human Cathelicidin (LL-37), a Multifunctional Peptide, is Expressed by Ocular Surface Epithelia and has Potent Antibacterial and Antiviral Activity.* **Gordon, Y Jerold, et al., et al.** 5, 2005, Current Eye Research, Vol. 30, pp. 385-94.
20. *A Carpet-Based Mechanism for Direct Antimicrobial Peptide Activity Against Vaccinia Virus Membranes.* **Dean, RE, et al., et al.** 11, 2010, Peptides, Vol. 31, pp. 1966-72.
21. *Selective Killing of Vaccinia Virus by LL-37: Implications for Eczema Vaccinatum.* **Howell, Michael D, et al., et al.** 3, 2012, Journal of Immunology, Vol. 172, pp. 1763-67.
22. *The Antimicrobial Peptide LL-37 Inhibits HIV-1 Replication.* **Bergman, Peter, et al., et al.** 4, 2007, Current HIV Research, Vol. 5, pp. 410-15.
23. *Anti-Adenoviral Effects of Human Cationic Antimicrobial Protein-18/LL-37, an Antimicrobial Peptide, by Quantitative Polymerase Chain Reaction.* **Uchio, Eiichi, Inoue, Hirotoshi and Kadonosono, Kazuaki.** 3, 2013, Korean Journal of Ophthalmology, Vol. 27, pp. 199-203.
24. *The Human Cathelicidin LL-37 has Antiviral Activity Against Respiratory Syncytial Virus.* **Currie, Silke M, et al., et al.** 8, 2013, PLoS One, Vol. 8.
25. *The Human Cathelicidin LL-37 Inhibits Influenza A Viruses Through a Mechanism Distinct From That of Surfactant Protein D or Defensins.* **Tripathi, Shweta, et al., et al.** 1, 2013, Journal of General Virology, Vol. 94, pp. 40-49.
26. *Effects of Cathelicidin and Its Fragments on Three key Enzymes of HIV-1.* **Wong, Jack Ho, et al., et al.** 6, s.l. : Peptides, 2011, Vol. 32.
27. *Beta-Defensins and LL-37 in Bronchoalveolar Lavage Fluid of Patients with Cystic Fibrosis.* **Chen, Christiane IU, et al., et al.** 1, 2004, Journal of Cystic Fibrosis, Vol. 3, pp. 45-50.
28. *Reduced Airway Surface pH Impairs Bacterial Killing in the Porcine Cystic Fibrosis Lung.* **Pezzulo, Alejandro A, et al., et al.** 7405, 2012, Nature, Vol. 487, pp. 109-13.
29. *LL-37 Complexation with Glycosaminoglycans in Cystic Fibrosis Lungs Inhibits Antimicrobial Activity, Which can be Restored by Hypertonic Saline.* **Bergsson, Gudmundur, et al., et al.** 1, 2009, Journal of Immunlogy, Vol. 183, pp. 543-51.
30. *Rational Design of alpha-Helical Antimicrobial Peptides with Enhanced Activities and Specificity/Therapeutic Index.* **Chen, Yuxin, et al., et al.** 13, 2005, Journal of Biological Chemistry, Vol. 280, pp. 12316-329.
31. *Design of a Novel Tryptophan-Rich Membrane-Active Antimicrobial Peptide from the Membrane-Proximal Region of the HIV Glycoprotein, gp41.* **Haney, Evan F, et al., et al.** 2012, Beilstein Journal of Organic Chemistry, Vol. 8, pp. 1172-84.
32. *Effect of Amino Acid Substitutions on Calmodulin Binding and Cytolytic Properties of the LLP-1 Peptide Segment of Human Immunodeficiency Virus Type 1 Transmembrane Protein.* **Tencza, Sarah B, et al., et al.** 8, 1995, Journal of Virology, Vol. 69, pp. 5199-202.

33. *Selective Toxicity of Engineered Lentivirus Lytic Peptides in a CF Airway Cell Model.* **Phadke, Shruti M, et al., et al.** 8, 2003, Peptides, Vol. 24, pp. 1099-107.
34. *Novel Antimicrobial Peptides Derived from Human Immunodeficiency Virus Type 1 and Other Lentivirus Transmembrane Proteins.* **Tencza, Sarah B, et al., et al.** 11, 1997, Antimicrobial Agents and Chemotherapy, Vol. 41, pp. 2394-98.
35. *De novo Generation of Cationic Antimicrobial Peptides: Influence of Length and Tryptophan Substitution on Antimicrobial Activity.* **Deslouches, Berthony, et al., et al.** 1, 2005, Antimicrobial Agents and Chemotherapy, Vol. 49, pp. 316-22.
36. *Tryptophan- and Arginine-Rich Antimicrobial Peptides: Structures and Mechanisms of Action.* **Chan, David I, Prenner, Elmar J and Vogel, Hans J.** 9, 2006, Biochimica et Biophysica Acta, Vol. 1758, pp. 1184-202.
37. *Towards a Structure-Function Analysis of Bovine Lactoferricin and Related Tryptophan- and Arginine-Containing Peptides.* **Vogel, HJ, et al., et al.** 1, 2002, Biochemistry and Cell Biology, Vol. 80, pp. 49-63.
38. *Tryptophan-Rich Antimicrobial Peptides: Comparative Properties and Membrane Interactions.* **Schibli, DJ, et al., et al.** 5, 2002, Biochemistry and Cell Biology, Vol. 80, pp. 667-77.
39. *Activity of the de novo Engineered Antimicrobial Peptide WLBU2 against Pseudomonas aeruginosa in Human Serum and Whole Blood: Implications for Systemic Implications.* **Deslouches, Berthony, et al., et al.** 8, 2005, Antimicrobial Agents and Chemotherapy, Vol. 49, pp. 3208-16.
40. *Rational Design of Engineered Cationic Antimicrobial Peptides Consisting Exclusively of Arginine and Tryptophan, and Their Activity against Multidrug-Resistant Pathogens.* **Deslouches, Berthony, et al., et al.** 6, 2013, Antimicrobial Agents and Chemotherapy, Vol. 57, pp. 2511-21.
41. *De novo-Derived Cationic Antimicrobial Peptide Activity in a Murine Model of Pseudomonas aeruginosa Bacteraemia.* **Deslouches, Berthony, et al., et al.** 3, 2007, Journal of Antimicrobial Chemotherapy, Vol. 60, pp. 669-72.
42. *Virus Entry, Assembly, Budding, and Membrane Rafts.* **Chazal, Nathalie and Gerlier, Denis.** 2, s.l. : Microbiology and Molecular Biology Reviews, 2003, Vol. 67.
43. *Cholesterol and the Interaction of Proteins with Membrane Domains.* **Epand, Richard M.** 4, 2006, Progress in Lipid Research, Vol. 45, pp. 279-94.
44. *Peripheral-Type Benzodiazepine Receptor Function in Cholesterol Transport. Identification of a Putative Cholesterol Recognition/Interaction Amino Acid Sequence and Consensus Pattern.* **Li, Hua and Papadopoulos, Vassilios.** 12, 1998, Endocrinology, Vol. 139, pp. 4991-97.
45. *Large Changes in the CRAC Segment of the gp41 of HIV Does Not Destroy Fusion Activity if the Segment Interacts with Cholesterol.* **Vishwanathan, Sundaram A, et al., et al.** 45, 2008, Biochemistry, Vol. 47, pp. 11869-876.
46. *Membrane-Proximal External HIV-1 gp41 Motif Adapted for Destabilizing the Highly Rigid Viral Envelope.* **Apellaniz, Beatriz, et al., et al.** 10, 2011, Biophysical Journal, Vol. 101, pp. 2426-35.
47. *Mechanism of Membrane Perturbation by the HIV-1 gp41 Membrane-Proximal External Region and its Modulation by Cholesterol.* **Ivankin, Andrey, et al., et al.** 11, 2012, Biochimica et Biophysica Acta, Vol. 1818, pp. 2521-28.

48. WHO Global Health Observatory HIV/AIDS. *World Health Organization.* [Online] May 7, 2014. http://www.who.int/gho/hiv/en/.
49. *Envelope Glycoprotein Incorporation, Not Shedding of Surface Envelope Glycoprotein (gp120/SU), is the Primary Determinant of SU Content of Purified Human Immunodeficiency Virus Type 1 and Simian Immunodeficiency Virus.* **Chertova, Elena, et al., et al.** 11, 2002, Journal of Virology, Vol. 76, pp. 5315-25.
50. *Evidence for Budding of Human Immunodeficiency Virus Type 1 Selectively from Glycolipid-Enriched Membrane Lipid Rafts.* **Nguyen, Dzung H and Hildreth, James EK.** 7, s.l. : Journal of Virology, 2000, Vol. 74.
51. *Lipid Composition and Fluidity of the Human Immunodeficiency Virus Envelope and Host Cell Plasma Membranes.* **Aloia, Roland C, Tian, Huirou and Jensen, Fred C.** s.l. : PNAS, 1993, Vol. 90.
52. *Modification of the Fatty Acid Composition of Cultured Human Fibroblasts.* **Spector, Arthur A, et al., et al.** 4, 1979, Journal of Lipid Research, Vol. 20, pp. 536-47.
53. *The HIV Lipidome: A Raft With an Unusual Composition.* **Brugger, Britta, et al., et al.** 8, s.l. : PNAS, 2006, Vol. 103.
54. *Roles of Human Immunodeficiency Virus Type 1 Membrane Cholesterol in Viral Internalization.* **Guyader, Mireille, et al., et al.** 20, 2002, Journal of Virology, Vol. 76, pp. 10356-364.
55. People at High Risk of Developing Flu–Related Complications. *Centers for Disease Control and Prevention.* [Online] [Cited: May 9, 2014.] http://www.cdc.gov/flu/about/disease/high_risk.htm.
56. *The Annual Impact of Season Influenza in the US: Measuring Disease Burden and Costs.* **Molinari, Noelle-Angelique M, et al., et al.** 25, s.l. : Vaccines, 2007, Vol. 25.
57. WHO Global Influenza Surveillance Network (GISN) Surveillance and Vaccine Development. *WHO Collaborating Centre for Reference and Research on Influenza.* [Online] [Cited: May 28, 2014.] http://www.influenzacentre.org/centre_GISN.htm.
58. *The Evolution of Epidemic Influenza.* **Nelson, Martha I and Holmes, Edward C.** s.l. : Nature Reviews Genetics, 2007, Vol. 8.
59. *Genesis of a Highly Pathogenic and Potentially Pandemic H5N1 Influenza Virus in Eastern Asia.* **Li, KS, et al., et al.** s.l. : Nature, 2004, Vol. 430.
60. Influenza Antiviral Medications: Summary for Clinicians. *Centers for Disease Control and Prevention.* [Online] [Cited: May 28, 2014.] http://www.cdc.gov/flu/professionals/antivirals/summary-clinicians.htm.
61. *Influenza A Viruses: New Research Developments.* **Medina, Rafael A and Garcia-Sastre, Adolfo.** s.l. : Nature Reviews Microbiology, 2011, Vol. 9.
62. *Influenza Viruses Select Ordered Lipid Domains During Budding From the Plasma Membrane.* **Scheiffele, Peter, et al., et al.** 4, s.l. : Journal of Biological Chemistry, 1999, Vol. 274.
63. *Role for Influenza Virus Envelope Cholesterol in Virus Entry and Infection.* **Sun, Xiangjie and Whittaker, Gary R.** 23, s.l. : Journal of Virology, 2003, Vol. 77.
64. *Structure and Accessibility of HA Trimers on Intact 2009 H1N1 Pandemic Influenza Virus to Stem-Region Specific Neutralizing Antibodies.* **Harris, Audray K, et al., et al.** 2013, PNAS.
65. WHO Global Alert and Response Impact of Dengue. *World Health Organization.* [Online] May 8, 2014. http://www.who.int/csr/disease/dengue/impact/en/.

66. *Epidemiology of Dengue: Past, Present and Future Prospects.* **Murray, Natasha EA, Quam, Mikkel B and Wilder-Smith, Annelies.** 2013, Clinical Epidemiology, Vol. 5, pp. 299-309.
67. *The Global Distribution and Burden of Dengue.* **Bhatt, Samir, et al., et al.** 7446, 2013, Nature, Vol. 496, pp. 504-7.
68. *Age and Clinical Dengue Illness.* **Egger, Joseph R and Coleman, Paul G.** 6, 2007, Emerging Infectious Diseases, Vol. 13, pp. 49-51.
69. *Structure of Dengue Virus: Implications for Flavivirus Organization, Maturation, and Fusion.* **Kuhn, Richard J, et al., et al.** 5, 2002, Cell, Vol. 108, pp. 717-25.
70. *Structure of Dengue Virus Envelope Protein After Membrane Fusion.* **Modis, Yorgo, et al., et al.** 6972, 2004, Nature, Vol. 427, pp. 313-19.
71. *Structural Proteomics of Dengue Virus.* **Perera, Rushika and Kuhn, Richard J.** 4, 2008, Current Opinion in Microbiology, Vol. 11, pp. 369-77.
72. *Caveolin-1 in Lipid Rafts Interacts with Dengue Virus NS3 During Polyprotein Processing and Replication in HMEC-1 Cells.* **Cordero, Julio G, et al., et al.** 3, 2014, PLoS One, Vol. 9.
73. *Requirement of Cholesterol in the Viral Envelope for Dengue Virus Infection.* **Carro, Ana C and Damonte, Elsa B.** 1-2, 2013, Virus Research, Vol. 174, pp. 78-87.
74. *A Coarse-Grained Protein Force Field for Folding and Structure Prediction.* **Maupetit, Julien, Tuffery, P and Derreumaux, Philippe.** 2, s.l. : Proteins, 2007, Vol. 69.
75. *PEP-FOLD: An Updated de novo Structure Prediction Server for Both Linear and Disulfide Bonded Cyclic Peptides.* **Thevenet, Pierre, et al., et al.** 2012, Nucleic Acids Research, Vol. 40, pp. W288-93.
76. *A Survey of Potential Problems and Quality Control in Peptide Synthesis by the Fluorenylmethoxycarbonyl Procedure.* **Fontenot, JD, et al., et al.** 1, 1991, Peptide Research, Vol. 4, pp. 19-25.
77. *Protein Secondary Structure Analyses from Circular Dichroism Spectroscopy: Methods and Reference Databases.* **Whitmore, Lee and Wallace, BA.** 5, 2007, Biopolymers, Vol. 89, pp. 392-400.
78. *Analysis of Protein Circular Dichroism Spectra for Secondary Structure Using a Simple Matrix Multiplication.* **Compton, Larry A and Johnson Jr, W Curtis.** 1, 1986, Analytical Biochemistry, Vol. 155, pp. 155-67.
79. *Variable Selection Method Improves the Prediction of Protein Secondary Structure from Circular Dichroism Spectra.* **Manavalan, Parthasarathy and Johnson Jr, W Curtis.** 1, 1987, Analytical Biochemistry, Vol. 167, pp. 76-85.
80. *Estimation of Protein Secondary Structure from Circualr Dichroism Spectra: Comparison of CONTIN, SELCON, and CDSSTR Methods with an Expanded Reference Set.* **Sreerama, Narasimha and Woody, Robert W.** 2, 2000, Analytical Biochemistry, Vol. 287, pp. 252-60.
81. *A Reference Database for Circular Dichroism Spectroscopy Covering Fold and Secondar Structure Space.* **Lees, Jonathan G, et al., et al.** 16, 2006, Bioinformatics, Vol. 22, pp. 1955-62.
82. *Replication and Plaque Assay of Influenza Virus in an Established Line of Canine Kidney Cells.* **Gaush, Charles R and Smith, Thomas F.** 4, s.l. : Applied Microbiology, 1968, Vol. 16.

83. *A Plaque Reduction Test for Dengue Virus Neutralizing Antibodies.* **Russell, Philip K, et al., et al.** 2, s.l. : Journal of Immunology, 1967, Vol. 99.
84. *Use of an Aqueous Soluble Tetrazolium/Formazan Assay for Cell Growth Assays in Culture.* **Cory, AH, et al., et al.** 7, s.l. : Cancer Communications, 1991, Vol. 3.
85. *Precision Relative Aggregation Number Determinations of SDS Micelles Using a Spin Probe. A Model of Micelle Surface Hydration.* **Bales, Barney L, et al., et al.** 50, s.l. : Journal of Physical Chemistry, 1998, Vol. 102.
86. *Rapid Colorimetric Assay for Cellular Growth and Survival: Application to Proliferation and Cytotoxicity Assays.* **Mosmann, Tim.** 1-2, 1983, Journal of Immunological Methods, Vol. 65, pp. 55-63.
87. *Comparative Transcriptome Profiling of an SV40-Transformed Human Fibroblast (MRC5CVI) and Its Untransformed Counterpart (MRC-5) in Response to UVB Irradiation.* **Chang, Cheng-Wei, et al., et al.** 9, 2013, PLoS One, Vol. 8.
88. *Use of MDCK Cells for Production of Live Attenuated Influenza Vaccine.* **Liu, Jonathan, et al., et al.** 46, 2009, Vaccine, Vol. 27, pp. 6460-63.
89. *Bovine Lactoferricin Selectively Induces Apoptosis in Human Leukemia and Carcinoma Cell Lines.* **Mader, Jamie S, et al., et al.** 4, 2005, Molecular Cancer Therapeutics, Vol. 4, pp. 612-24.
90. *The Antimicrobial Peptide, Lactroferricin B, is Cytotoxic to Neuroblastoma Cells in vitro and Inhibits Xenograft Growth invitro.* **Eliassen, Liv T, et al., et al.** 3, 2006, International Journal of Cancer, Vol. 119, pp. 493-500.
91. *Membrane Fluidity Characteristics of Human Lung Cancer.* **Sok, Miha, Sentjure, Marjeta and Schara, Milan.** 2, 1999, Cancer Letters, Vol. 139, pp. 215-20.
92. *Influence of Membrane Fluidity on Human Immunodeficiency Virus Type 1 Entry.* **Harada, Shinji, et al., et al.** 2, s.l. : Biochemical and Biophysical Research Communications, 2005, Vol. 329.
93. *Semen-Derived Amyloid Fibrils Dranstically Enhance HIV Infection.* **Munch, Jan, et al., et al.** 6, 2007, Cell, Vol. 131, pp. 1059-71.
94. *The Cationic Properties of SEVI Underlie its Ability to Enhance Human Immunodeficiency Virus Infection.* **Roan, Nadia R, et al., et al.** 1, 2009, Journal of Virology, Vol. 83, pp. 73-80.
95. *Evolving Complexities of Influenza Virus and its Receptors.* **Nicholls, John M, et al., et al.** 4, s.l. : Trends in Microbiology, 2008, Vol. 16.
96. *Mutation of the Dengue Virus Type 2 Envelope Protein Heparan Sulfate Binding Sites or the Domain III Lateral Ridge Blocks Replication in Vero Cells Prior to Membrane Fusion.* **Roehrig, John T, et al., et al.** 2, s.l. : Virology, 2013, Vol. 441.
97. *Relationships Between Infectious Titer, Capsid Protein Levels, and Reverse Transcriptase Activities of Diverse Human Immunodeficiency Virus Type 1 Isolates.* **Marozsan, Andre J, et al., et al.** 20, s.l. : Journal of Virology, 2004, Vol. 78.
98. *Mutational Analysis of cis-Acting RNA Signals in Segment 7 of Influenza A Virus.* **Hutchinson, Edward C, et al., et al.** 23, s.l. : Journal of Virology, 2008, Vol. 82.
99. *Quantitative Analysis of Dengue-2 Virus RNA During the Extrinsic Incubation Period in Individual Aedes aegypti.* **Richardson, Jason, et al., et al.** 1, s.l. : American Journal of Tropical Medicine and Hygiene, 2006, Vol. 74.
100. *Cholesterol and the Cell Membrane.* **Yeagle, PL.** 3-4, s.l. : Biochimica et Biophysica Acta, 1985, Vol. 822.

101. *Decreased Erythrocyte Membrane Fluidity and Altered Lipid Composition in Human Liver Disease*. **Owen, James S, et al., et al.** s.l. : Journal of Lipid Research, 1982, Vol. 23.
102. *Total Cholesterol Content of Erythrocyte Membranes is Associated with the Severity of Coronary Artery Disease and the Therapeutic Effect of Rosuvastatin.* **Zhong, Yucheng, et al., et al.** 4, s.l. : Informa Health Care, 2012, Vol. 117.
103. *On the Mechanism of Transfer of Cholesterol Between Human Erythrocytes and Plasma.* **Lange, Yvonne, et al., et al.** 11, s.l. : Journal of Biological Chemistry, 1983, Vol. 258.
104. *Tetrazolium Dyes as Tools in Cell Biology: New Insights into Their Cellular Reduction.* **Berridge, Michael V, Herst, Patries M and Tan, An S.** 2005, Biotechnology Annual Review, Vol. 11, pp. 127-52.
105. *The Challenges of Eliciting Neutralizing Antibodies to HIV-1 and to Influenza Virus.* **Hedestam Karlsson, Gunilla B, et al., et al.** s.l. : Nature Reviews Microbiology, 2008, Vol. 6.
106. Flavivirus. *ViralZone.* [Online] Swiss Institute of Bioinformatics. [Cited: May 18, 2014.] http://viralzone.expasy.org/all_by_species/24.html.